Sub-Riemannian Problems on 3D Lie Groups with Applications to Retinal Image Processing

A.P. Mashtakov TU/e

EU-Marie Curie FP7-PEOPLE-2013-ITN, MANET TU/e (no. 607643)

R. Duits, Yu.L. Sachkov, G.R. Sanguinetti, E.J. Bekkers, I. Beschastnyi

Promotor: Bart ter Haar Romeny

Funded by
the European Union

International Conference on

Mathematical Control Theory and Mechanics

Suzdal, Russia, July 3 – 7, 2015

Structure of the talk

- Motivation: Application in medical imaging
- Image analysis on Lie groups
- Sub-Riemannian problems on 3D Lie groups (short overview)
- **Sub-Riemannian problem in SE(2) with given external cost**
- **Sub-Riemannian problem in SO(3) with cuspless spherical projection constraint**

Motivation:
Computer Aided Diagnosis
system for early detection and
prevention of diabetic retinopathy

Analysis of Images of the Retina

Diabetic retinopathy --- one of the main causes of blindness.
Epidemic forms: 10% people in China suffer from DR.
Patients are found early --> treatment is well possible.
Early warning --- leakage and malformation of blood vessels.
The retina --- excellent view on the microvasculature of the brain.

Healthy retina

Diabetes Retinopathy with tortuous vessels

Detect Vascular Tree in Images of the Retina

Application: Early diagnosis of diabetes

Problem: Low contrast & crossings & bifurcations & scales

Aim: Reliable tracking of *all* blood vessels in retina

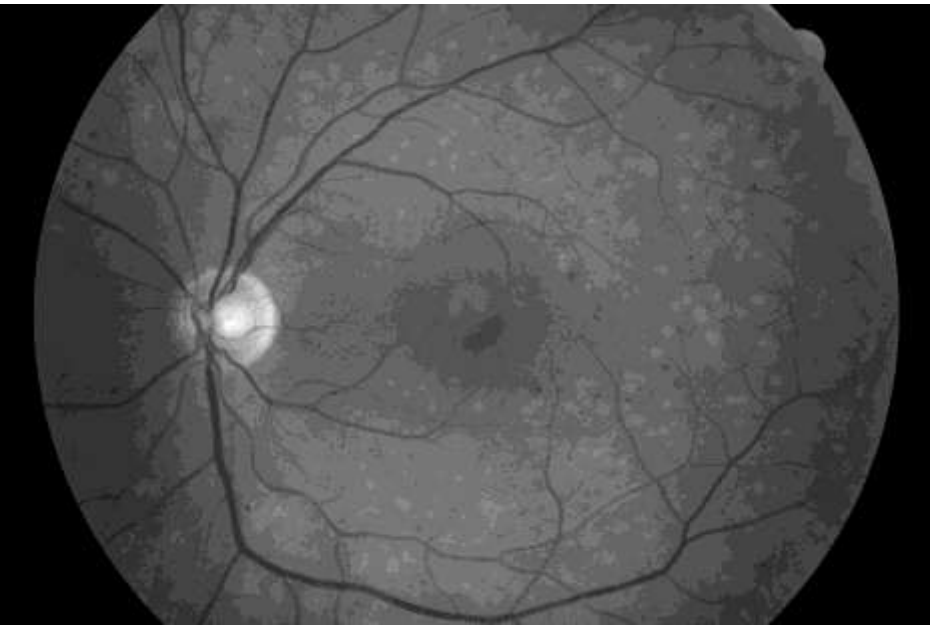

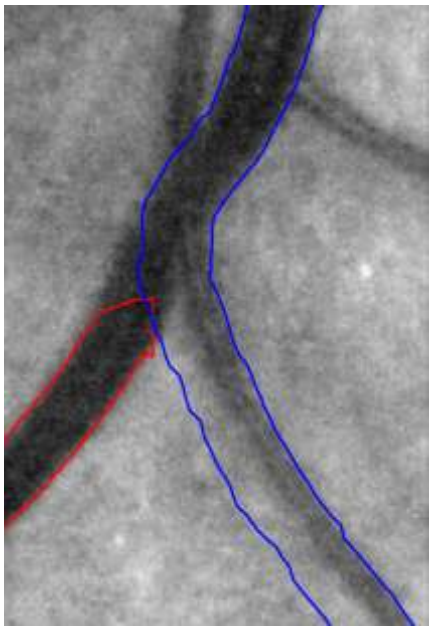

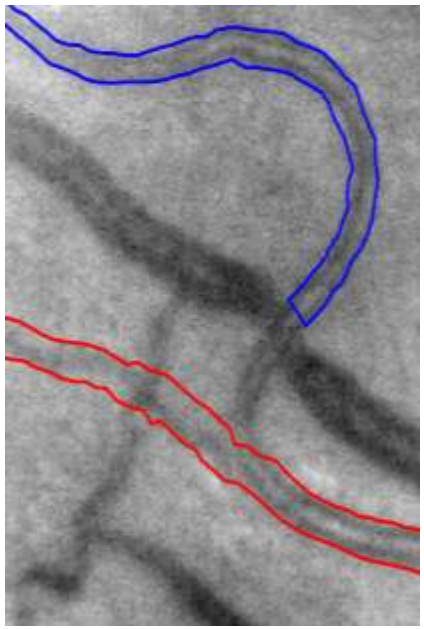

Sub-Riemannian Geodesics

We use data-driven sub-Riemannian geodesics for detection and analysis of blood vessel structure in optical images of the retina.

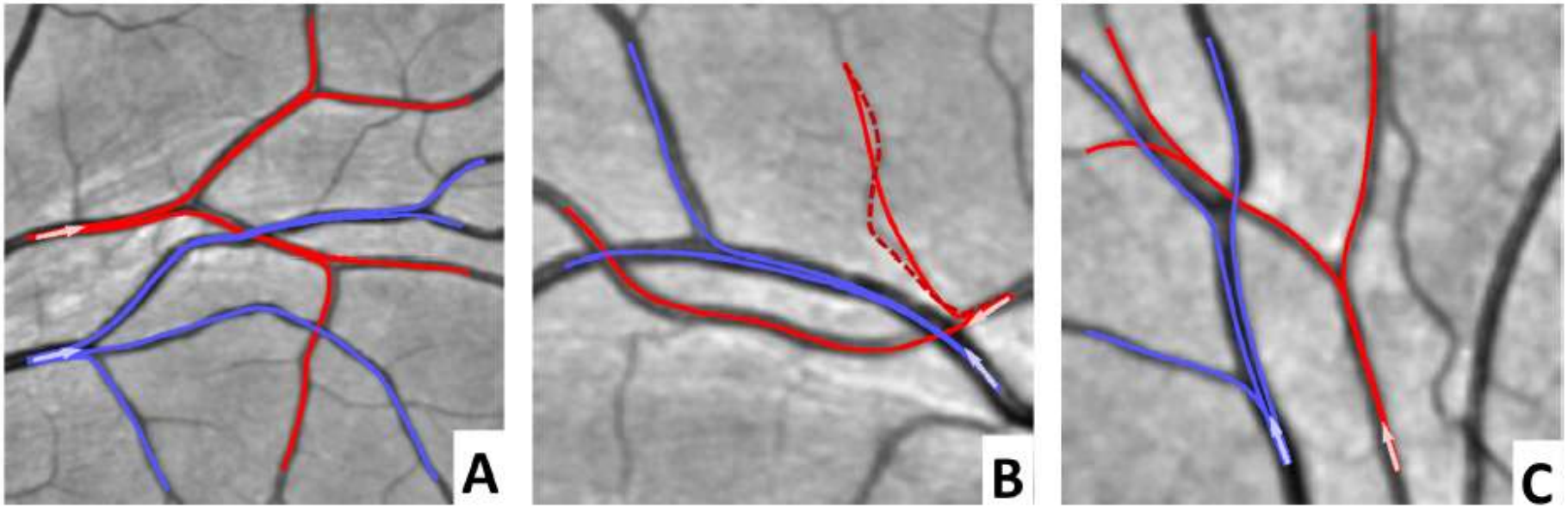

Lie groups image analysis

Contextual Image Analysis

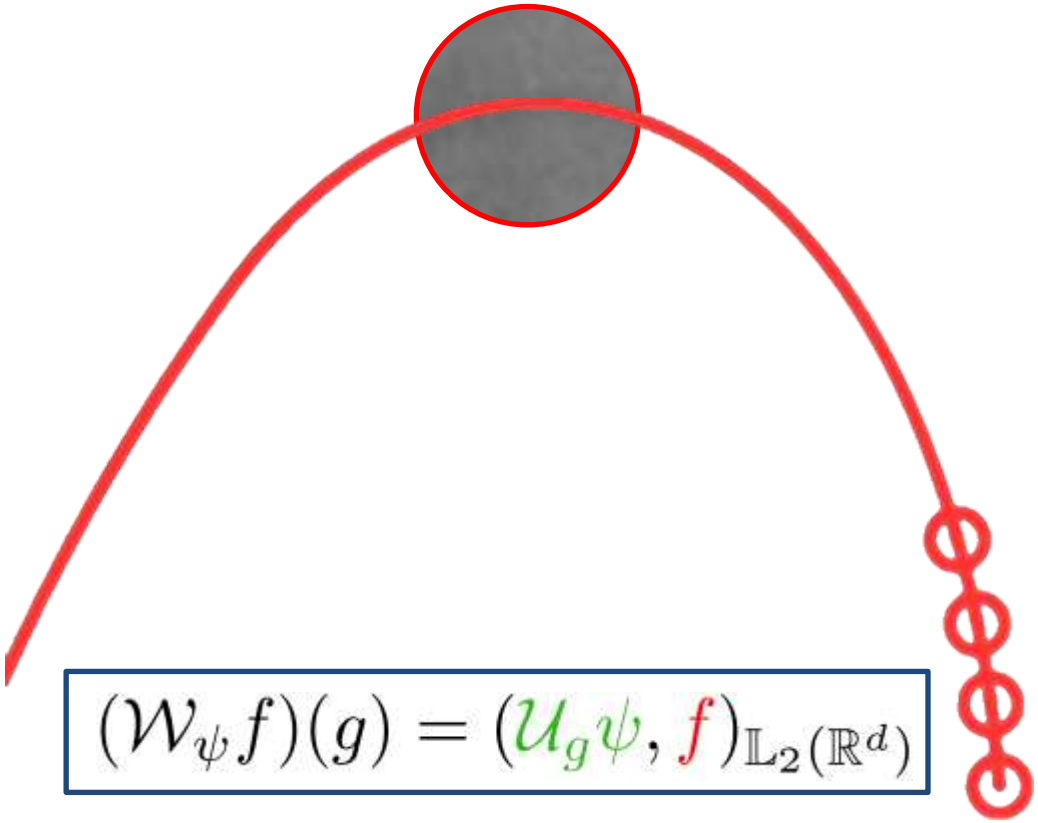

$$(\mathcal{W}_\psi f)(g) = (\mathcal{U}_g \psi, f)_{\mathbb{L}_2(\mathbb{R}^d)}$$

R. Duits: generic mathematical model for contextual image analysis via scores on Lie groups with many applications.

Lie Group Analysis via Invertible Orientation Scores

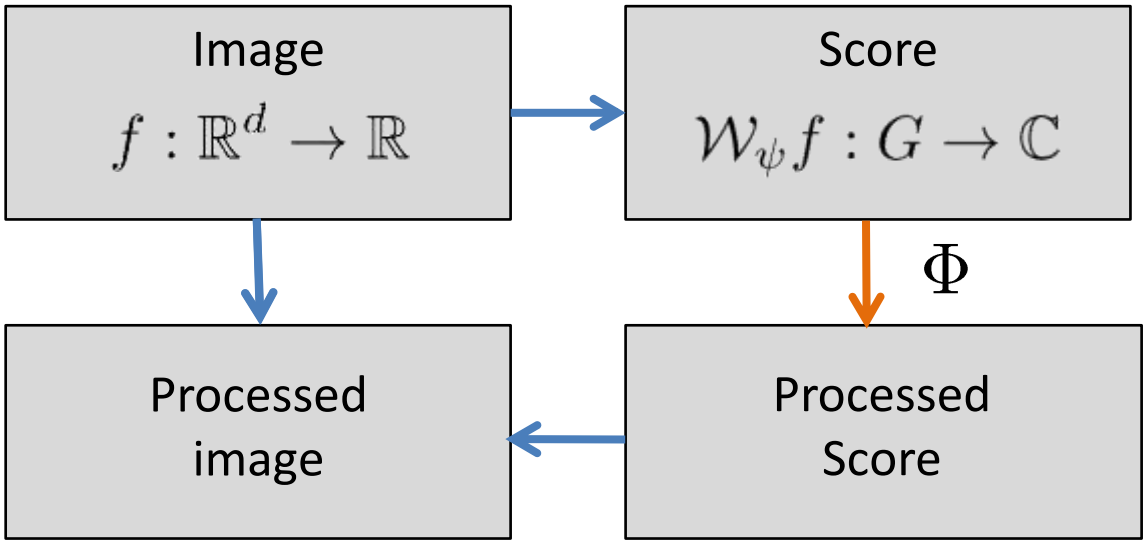

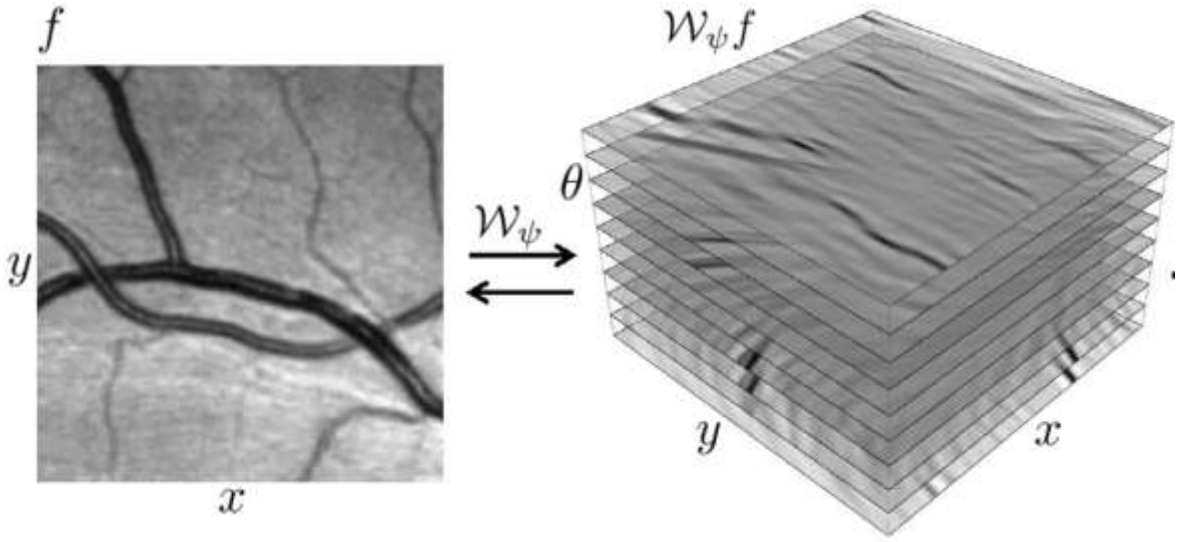

Application of 3D Lie Groups in Image Analysis

- Group of roto-translations of Euclidean plane SE(2): processing of flat images
- Group of rotations of Euclidean 3-dimensional space SO(3): processing of spherical images

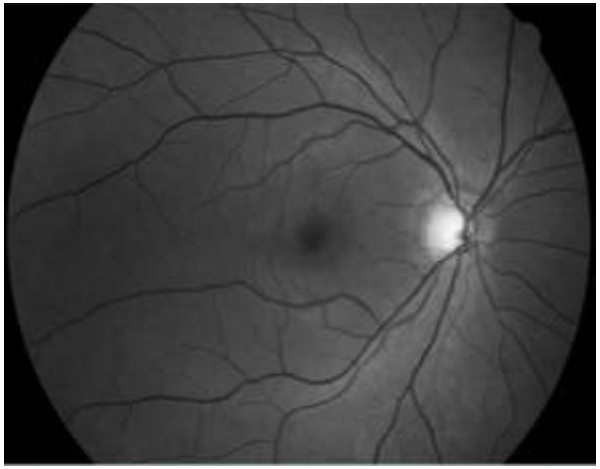

Sub-Riemannian problems on unimodular 3D Lie groups

Left-invariant sub-Riemannian structures

- G - 3D Lie group,
  L - Lie algebra of left-invariant vector fields on G,
  $\Delta \subset TG$, $\Delta + [\Delta, \Delta] = TG$ - left invariant subbundle,
  g - left-invariant inner product in Δ.

- Left-invariant contact sub-Riemannian structure on Lie group:

  $$(G, \Delta, g), \ \Delta = \operatorname{span}(X_1, X_2), \ g(X_i, X_j) = \delta_{ij}, \text{ where } X_1, X_2 \in L.$$

- Here X_1, X_2 are left-invariant vector fields on a 3D Lie group G, such that the distribution Δ is bracket-generating:

  $$\operatorname{span}(X_1(q), X_2(q), [X_1, X_2](q)) = T_qG, \quad q \in G.$$

- SR length minimizers $q : [0, t_1] \to G$, $\dot{q}(t) \in \Delta_{q(t)}$,

$$l(q(\cdot)) = \int_0^{t_1} \sqrt{g(\dot{q}(t), \dot{q}(t))}\, dt \to \min.$$

Classification of SR structures on 3D Lie groups

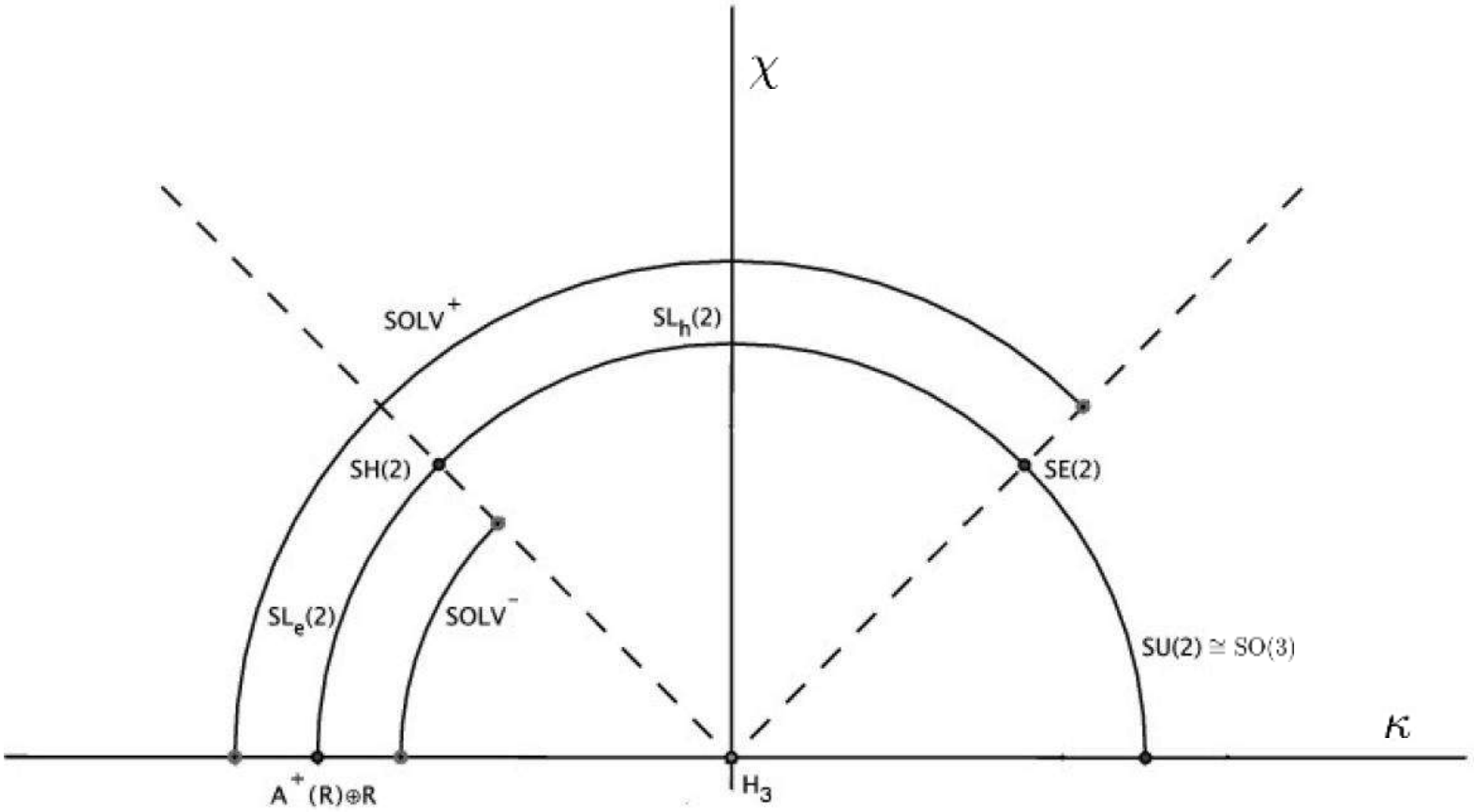

A. Agrachev, D. Barilari (2012):
Complete classification of left-invariant sub-Riemannian structures on 3D Lie groups in terms of the basic differential invariants κ and χ.

$$[X_2, X_1] = X_0,\ [X_1, X_0] = (\chi + \kappa)X_2,\ [X_2, X_0] = (\chi - \kappa)X_1$$

Optimal Control Problem

- Statement of the problem

$$\dot{q} = u_1 X_1(q) + u_2 X_2(q), \qquad q \in G, \qquad (u_1, u_2) \in \mathbb{R}^2,$$
$$q(0) = \mathrm{Id}, \qquad q(t_1) = q_1,$$
$$l = \int_0^{t_1} \sqrt{u_1^2 + u_2^2}\, dt \to \min,$$

- By Cauchy-Schwarz inequality: $J = \int_0^T \frac{u_1^2+u_2^2}{2}\, dt \to \min\,.$

ODE-based Approach to Optimal Control Problem

1. Existence of SR length minimizers (optimal trajectories),
2. Parametrization of SR geodesics (extremal trajectories) via PMP,
3. Selection of SR length minimizers among SR geodesics (study optimality of extremal trajectories).

Pontryagin Maximum Principle

- Pontryagin function:

$$H(\psi_0, \psi, q, u) = \psi_0 \frac{u_1^2 + u_2^2}{2} + \langle \psi, u_1 X_1 + u_2 X_2 \rangle,$$

where $\psi_0 \in \{0, -1\}$, $\psi = (\psi_1, \psi_2, \psi_3) \neq (0, 0, 0)$ – momentum variables,

- Maximality condition:

$$\mathbf{H}(\psi_0, \psi, \tilde{q}, \tilde{u}) = \max_{u \in \mathrm{R}^2} H(\psi_0, \psi, \tilde{q}, u),$$

where $(\tilde{q}, \tilde{u})$ is an optimal process,

- Hamiltonian system of PMP:

$$\dot{\psi} = -\frac{\partial \mathbf{H}}{\partial q}, \qquad \text{(vertical part)}$$

$$\dot{q} = \frac{\partial \mathbf{H}}{\partial \psi}. \qquad \text{(horizontal part)}$$

PMP in Moving Frame of References

Abnormal extremal trajectories ($\psi_0 = 0$): $u_i = 0$.

Normal extremal trajectories ($\psi_0 = -1$):

- Left invariant hamiltonians $h_i(\lambda) = \langle \psi, X_i(q) \rangle$, where $\lambda = (\psi, q) \in T^\star G$;
- Maximality condition: $u_i = h_i$;
- Hamiltonian $\mathrm{H} = \frac{1}{2}(h_1^2(\lambda) + h_2^2(\lambda))$;
- Normal Hamiltonian system of PMP:

$\dot{\lambda} = \vec{\mathrm{H}}(\lambda)$, where $\vec{\mathrm{H}}$ is the Hamiltonian vector field corresponding to H.

$$\begin{cases} \dot{h}_1 = h_2 h_0, \\ \dot{h}_2 = -h_1 h_0, \\ \dot{h}_0 = 2\chi h_1 h_2, \\ \dot{q} = h_1 X_1 + h_2 X_2. \end{cases}$$

H is an integral of the system.

Vertical Part of the Hamiltonian System

$$\begin{cases} \dot{h}_1 = h_2 h_0, \\ \dot{h}_2 = -h_1 h_0, \\ \dot{h}_0 = 2\chi h_1 h_2. \end{cases}$$

$$\Updownarrow$$

$$\begin{cases} \dot{r} = 0, \\ \dot{\nu} = c, \\ \dot{c} = -2\chi r^2 \sin\nu. \end{cases}$$

Mathematical Pendulum

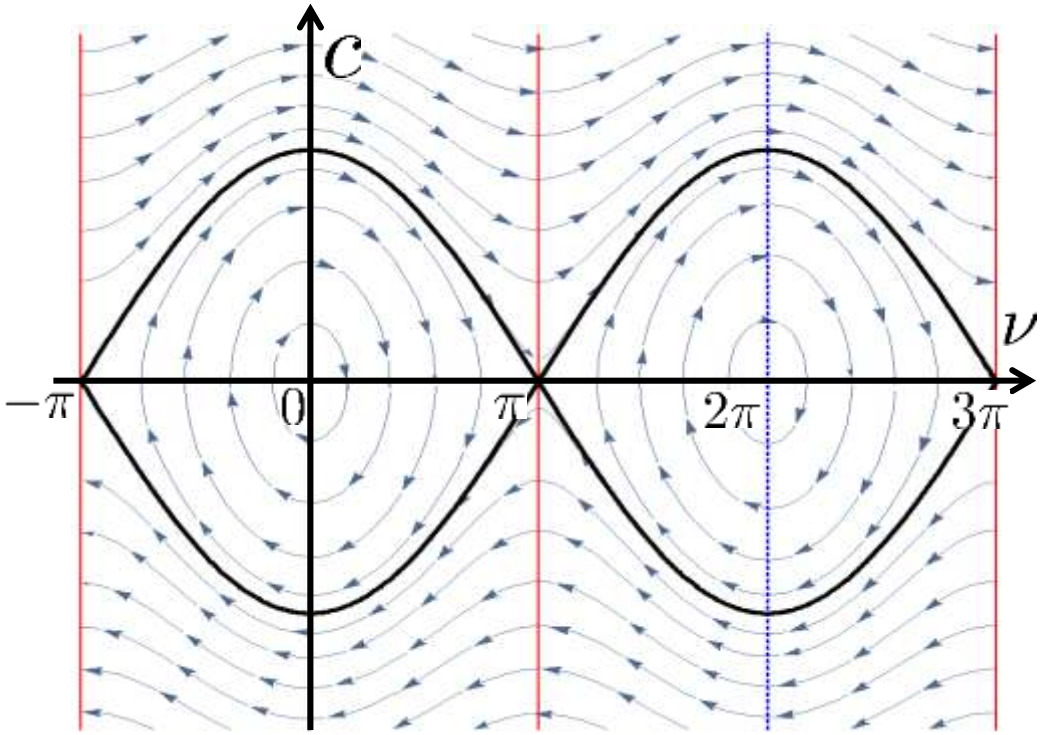

Horizontal Part -> Extremal Trajectories

Exponential mapping:

$$\mathrm{Exp} : (\lambda_0, t) = (\nu_0, c_0, t) \mapsto q(t)$$

Optimality of Extremal Trajectories

- Short arcs of extremal trajectories $q(s)$ are optimal
- Cut time along $q(s)$:

$$t_{cut} = \sup\{t > 0 \mid q(s),\ s \in [0,t],\ \text{ is optimal }\}.$$

- Maxwell time:

$$\exists\ \tilde{q}(s) \not\equiv q(s), \quad q(0) = \tilde{q}(0) = q_0,$$
$$q(t) = \tilde{q}(t) \text{ Maxwell point},$$
$$t = t_{MAX} \text{ Maxwell time}.$$

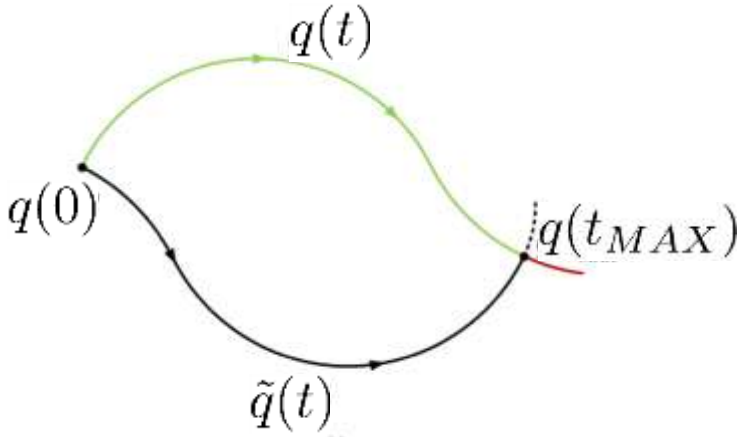

Maxwell Point

- Conjugate time:

q_{conj} – conjugate point $\Leftrightarrow$
q_{conj} critical value of Exp:
$\frac{\partial q(x,y,\theta)}{\partial \lambda} = 0$
conjugate time $q(t_{conj}) = q_{conj}$

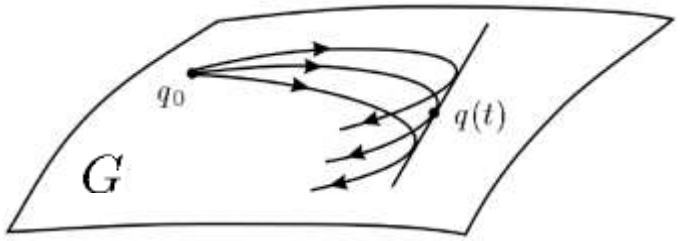

Conjugate Point

- Cut time:

$$t_{cut} = \min(t_{MAX}, t_{conj}).$$

Sub-Riemannian Wave Front

$$W(T) = \{\mathrm{Exp}(\lambda_0, T) | \lambda_0 \in T^*_{\mathrm{Id}}G, \mathrm{H}(\lambda_0) = \tfrac{1}{2}\}.$$

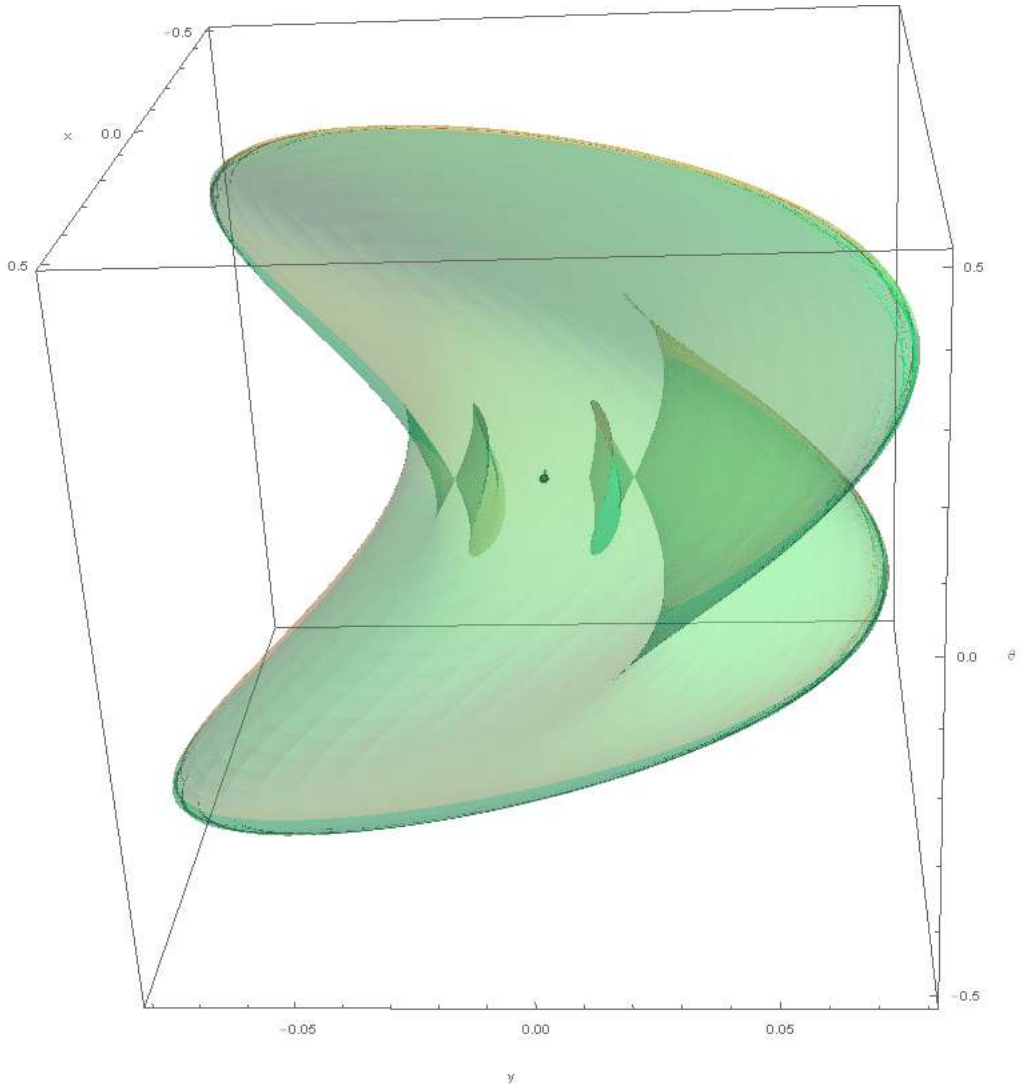

$\lambda_0 = (\nu_0, c_0)$

Varying t
$\Rightarrow$
one geodesic

Sub-Riemannian Wave Front

$$W(T) = \{\mathrm{Exp}(\lambda_0, T) | \lambda_0 \in T^*_{\mathrm{Id}}G, \mathrm{H}(\lambda_0) = \tfrac{1}{2}\}.$$

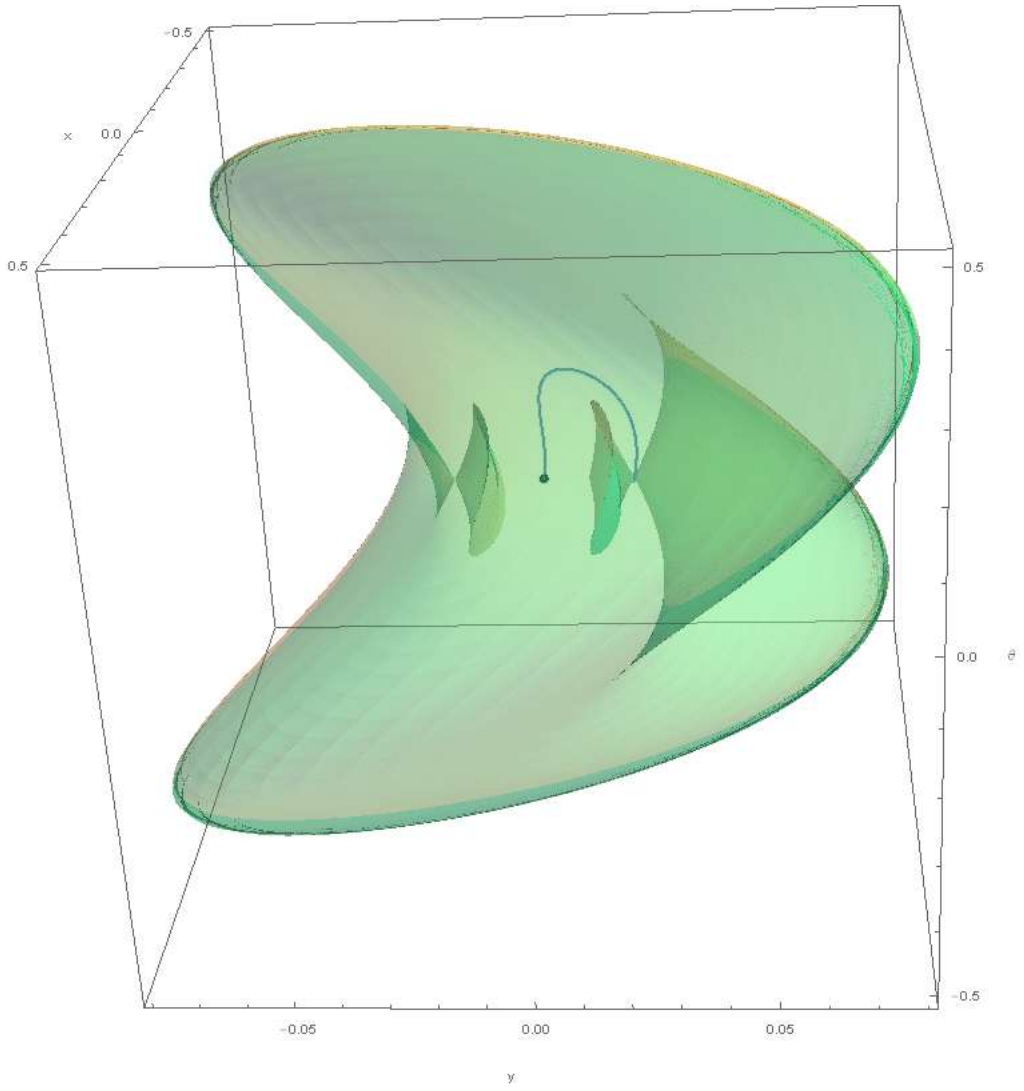

$\lambda_0 = (\nu_0, c_0)$

$t \in [0, T]$
Varying ν_0
$\Rightarrow$ family of geodesics

Sub-Riemannian Wave Front

$$W(T) = \{\mathrm{Exp}(\lambda_0, T) | \lambda_0 \in T^*_{\mathrm{Id}}G, \mathrm{H}(\lambda_0) = \tfrac{1}{2}\}.$$

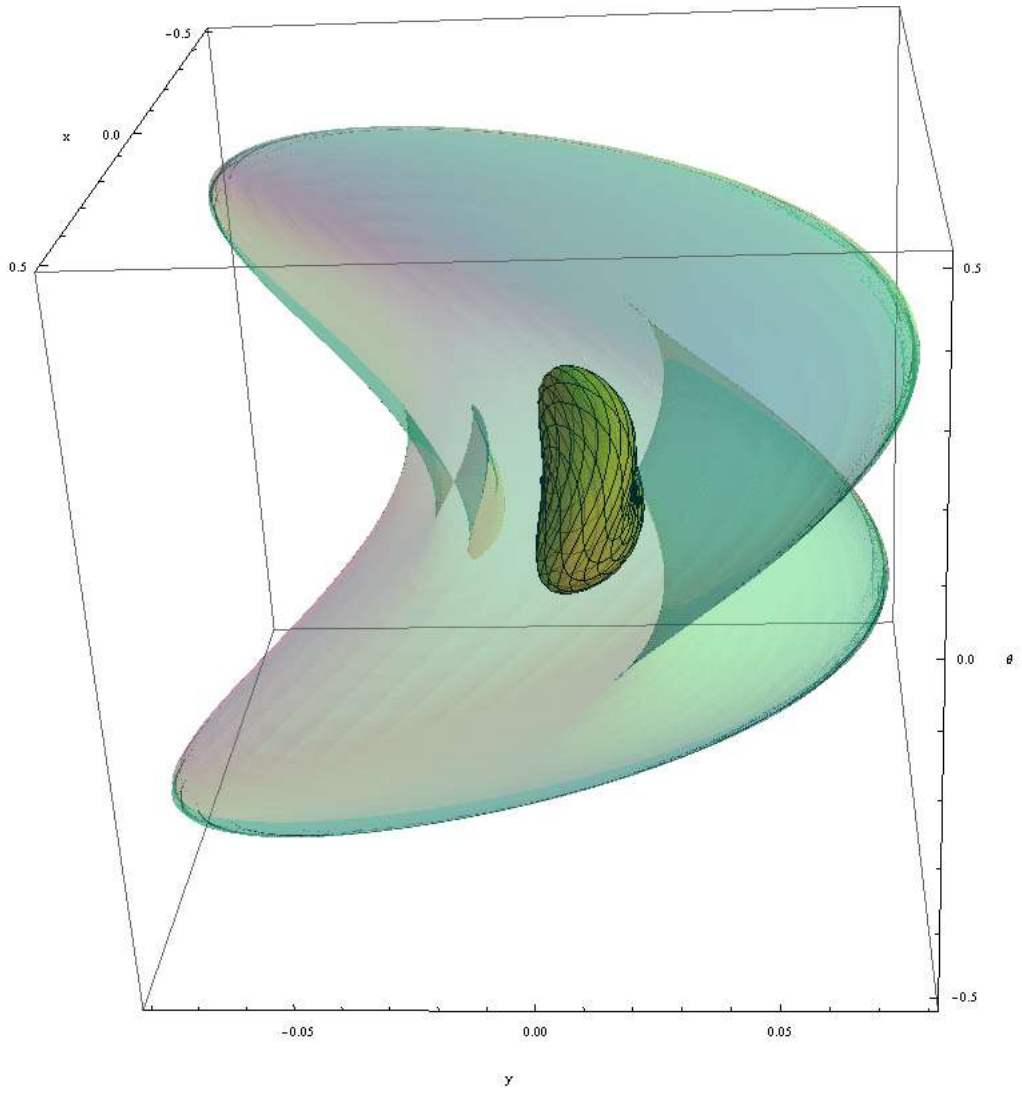

$$\lambda_0 = (\nu_0, c_0)$$

$$t \in [0, T]$$
$$2\nu_0 \in S^1$$

Varying c_0
$\Rightarrow$
whole family
of geodesics

Self intersection of Sub-Riemannian Wave Front

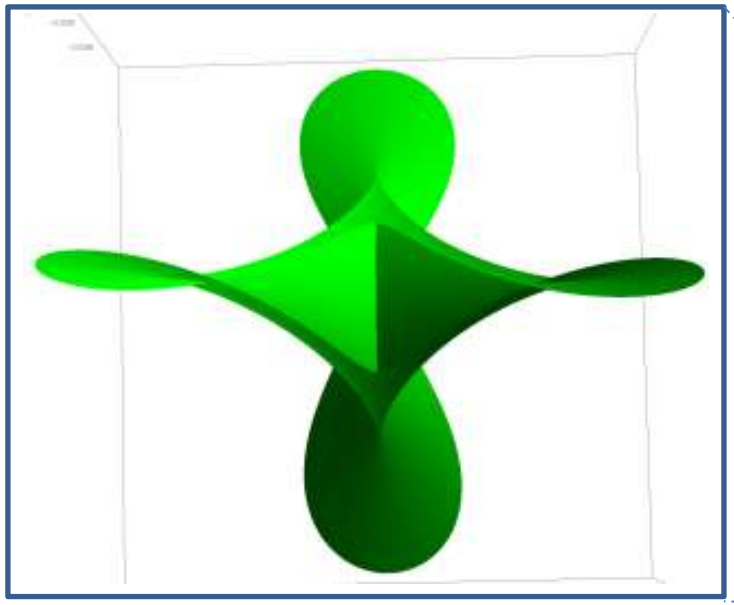

General case: astroidal shape of conjugate locus

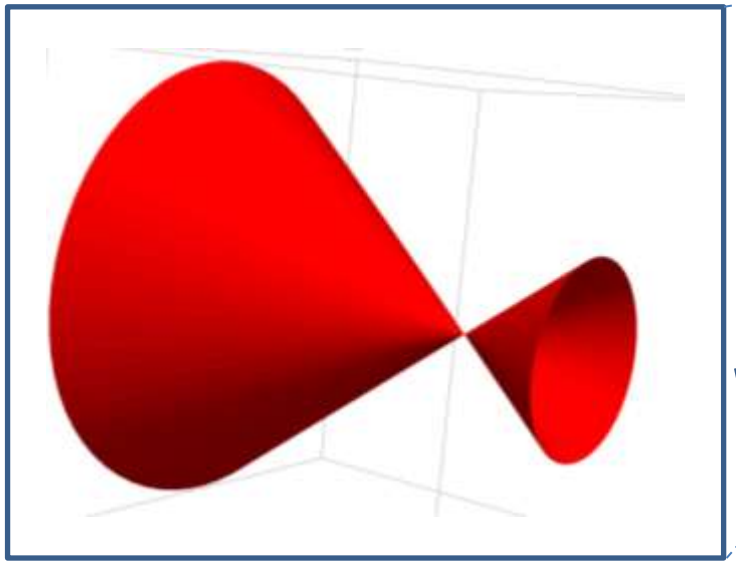

Special case with rotational symmetry

A.Agrachev…. H. Chakir, J.P. Gauthier and I. Kupka, Small Subriemannian Balls on R3. JDCS, 1996.

Sub-Riemannian Sphere

$$S(T) = \{\mathrm{Exp}(\lambda_0, T) | \lambda_0 \in T^*_{\mathrm{Id}} G, \mathrm{H}(\lambda_0) = \tfrac{1}{2}, t_{cut}(\lambda_0) \geq T\}.$$

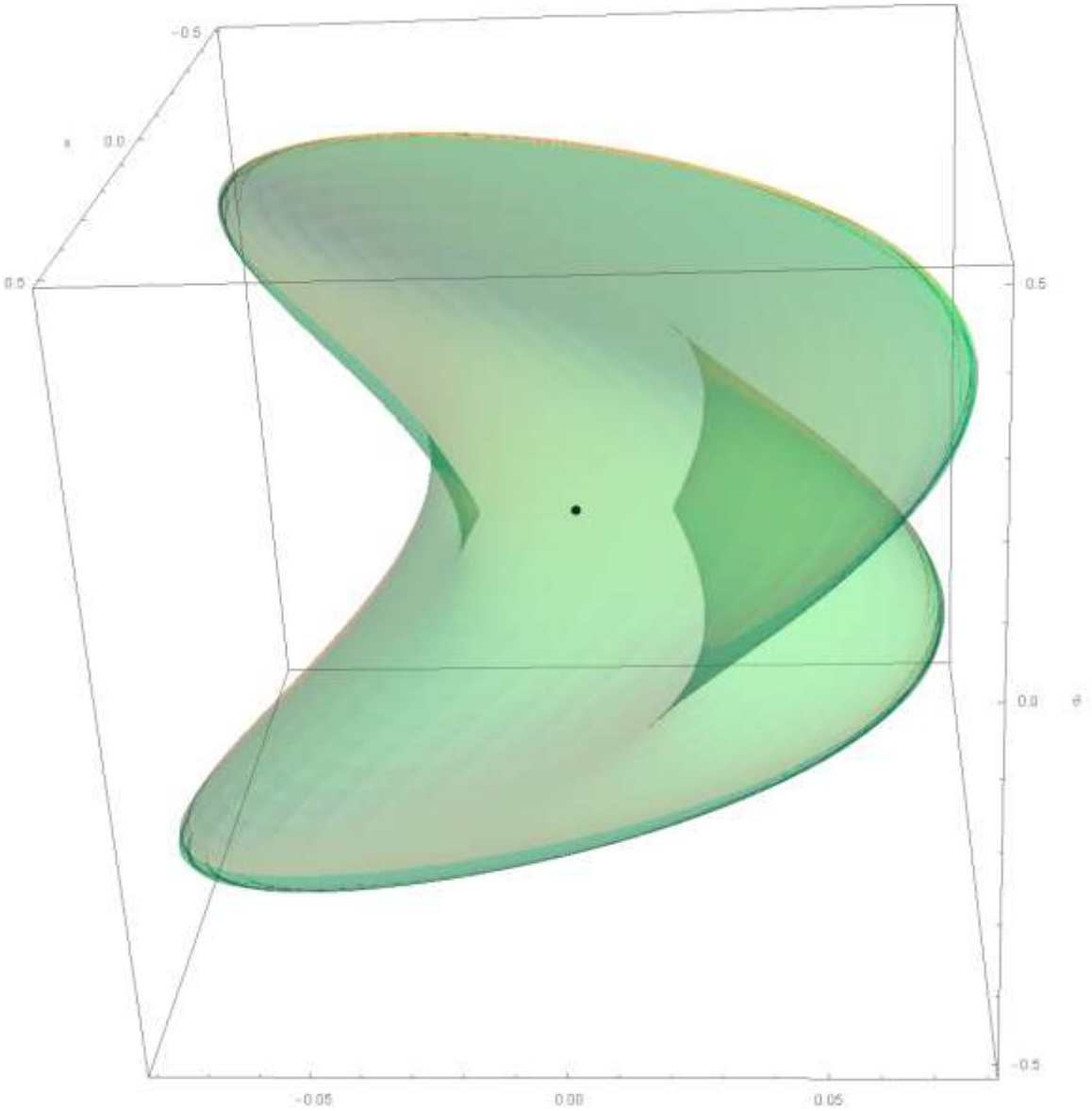

PDE-based Approach to Optimal Control Problem

Numerical scheme based on Hamilton-Jacobi-Bellman PDE:

- Derivation of HJB equation that describe wave front propagation from identity of the group;
- Constructing the distance map (based on viscosity solution of HJB equation);
- Computing optimal trajectories by steepest descent on the distance map.

Advantage: It allows extension to non-uniform data-driven cost

Sub-Riemannian problem in SE(2) with given external cost

(E.J. Bekkers, R. Duits, A. Mashtakov, G. Sanguinetti)

SE(2): Group of Roto-translations of a Plane

The group of Euclidean motions (rototranslations) of the plane:

$$\mathrm{SE}(2) = \left\{ \begin{pmatrix} \cos\theta & -\sin\theta & x \\ \sin\theta & \cos\theta & y \\ 0 & 0 & 1 \end{pmatrix} \mid \theta \in S^1,\ x, y \in \mathbb{R} \right\} \cong \mathbb{R}^2_{x,y} \ltimes S^1_\theta.$$

Lie algebra $\mathrm{se}(2) = T_{\mathrm{Id}}\,\mathrm{SE}(2) = \mathrm{span}(A_1, A_2, A_3)$,

$$A_1 = \begin{pmatrix} 0 & 0 & 1 \\ 0 & 0 & 0 \\ 0 & 0 & 0 \end{pmatrix}, \quad A_2 = \begin{pmatrix} 0 & -1 & 0 \\ 1 & 0 & 0 \\ 0 & 0 & 0 \end{pmatrix}, \quad A_3 = \begin{pmatrix} 0 & 0 & 0 \\ 0 & 0 & 1 \\ 0 & 0 & 0 \end{pmatrix}.$$

Lie algebra of left-invariant vector fields $\mathrm{L} = \mathrm{span}(X_1, X_2, X_3)$

$$X_1(q) = qA_1, \quad X_2(q) = qA_2, \quad X_3(q) = qA_3, \quad q \in \mathrm{SE}(2)\,.$$

Via the isomorphism $\mathrm{SE}(2) \cong \mathbb{R}^2_{x,y} \ltimes S^1_\theta$

$$X_1 \sim \mathcal{A}_1 = \cos\theta\partial_x + \sin\theta\partial_y, \quad X_2 \sim \mathcal{A}_2 = \partial_\theta, \quad X_3 \sim \mathcal{A}_3 = -\sin\theta\partial_x + \cos_\theta\,\partial_y.$$

Left-invariant Sub-Riemannian Problem on SE(2)

$$\dot{\gamma} = u^1 \mathcal{A}_1|_\gamma + u^2 \mathcal{A}_2|_\gamma,$$
$$\gamma(0) = \mathrm{Id}, \qquad \gamma(T) = g,$$
$$l(\gamma(\cdot)) = \int_0^T \sqrt{\xi^2 |u^1(t)|^2 + |u^2(t)|^2}\, \mathrm{d}t \to \min,$$
$$\gamma(t) \in \mathrm{SE}(2), \quad (u^1(t), u^2(t)) \in \mathbb{R}^2, \quad \xi > 0.$$

Was solved in recent works:

- I. Moiseev, Yu. L. Sachkov, Maxwell strata in sub-Riemannian problem on the group of motions of a plane, (2010)
- Yu. L. Sachkov, Conjugate and cut time in sub-Riemannian problem on the group of motions of a plane, (2010)
- Yu. L. Sachkov, Cut locus and optimal synthesis in the sub-Riemannian problem on the group of motions of a plane, (2011) (ESAIM:COCV)

Applications: Cortical Based Model of Perceptual Completion

- Sub-Riemanian structures in neurogeometry of the vision:
  - G. Citti and A. Sarti, A Cortical Based Model of Perceptual Completion in the Roto-Translation Space, 2006.
  - J. Petitot, The neurogeometry of pinwheels as a sub-Riemannian contact structure, 2003
- Variational principle: recovered arc should have minimal length in the space (x, y, θ):

$$\int \sqrt{\xi^2 \left(\dot{x}^2 + \dot{y}^2\right) + \dot{\theta}^2} dt \to \min .$$

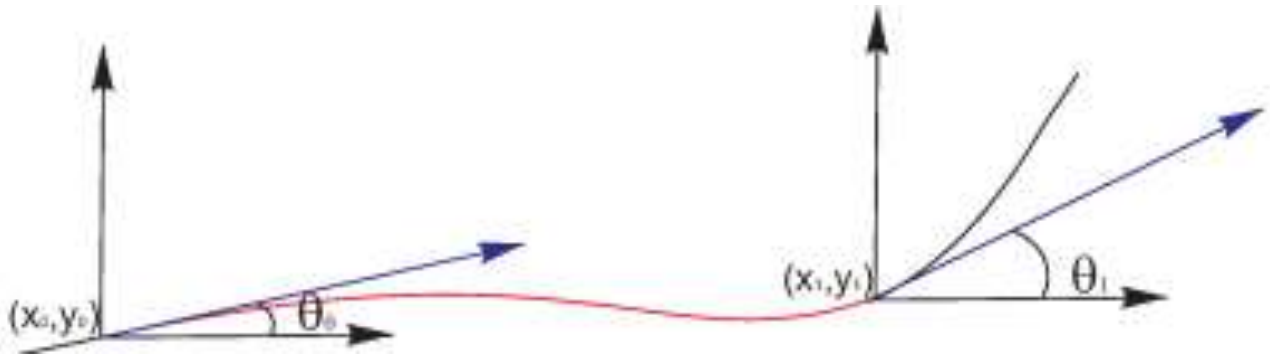

Application of SR minimizers in Image Analysis

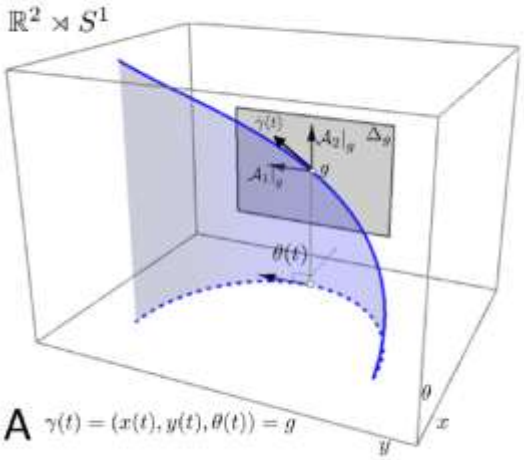

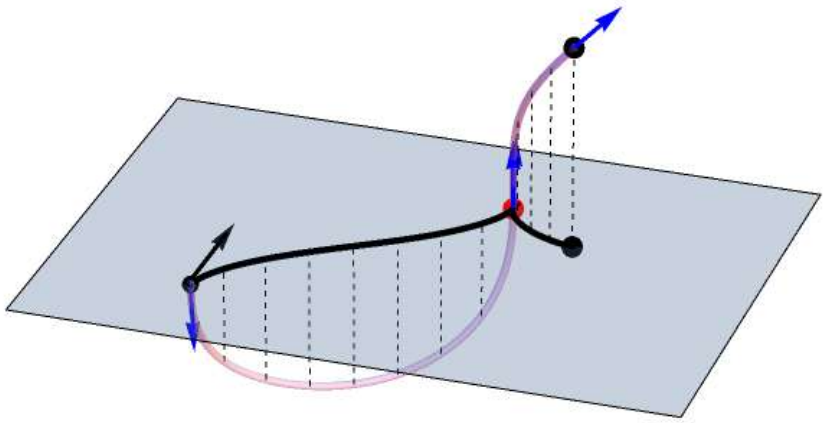

+ Disentanglement of intersecting structures,
+ Human brain inspired method for contour completion,

- Existence of cusp points

Cuspless Sub-Riemannian Geodesics in SE(2)

$\mathbf{P}_{\mathrm{Curve}}(\mathbb{R}^2)$:

$$\int_0^\ell \sqrt{\kappa^2+\xi^2}\mathrm{d}s$$
$$(\rightarrow \min, \ell \text{ free })$$
$$\mathbf{x}(0)=\mathbf{0}, \quad \mathbf{x}(\ell)=\mathbf{x}_{fin}$$
$$\theta(0)=0, \quad \theta(\ell)=\theta_{fin}$$

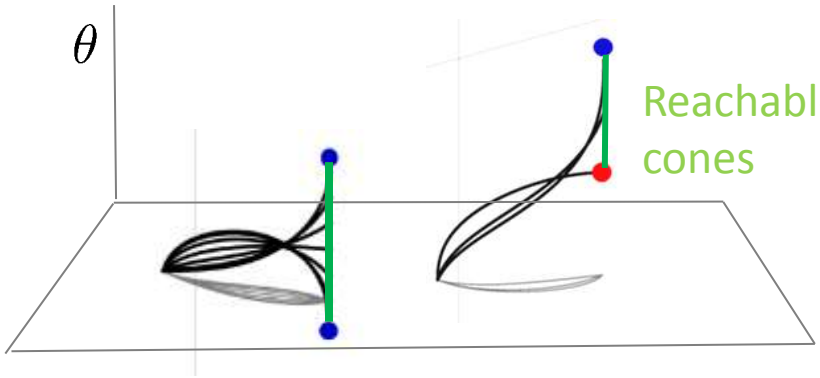

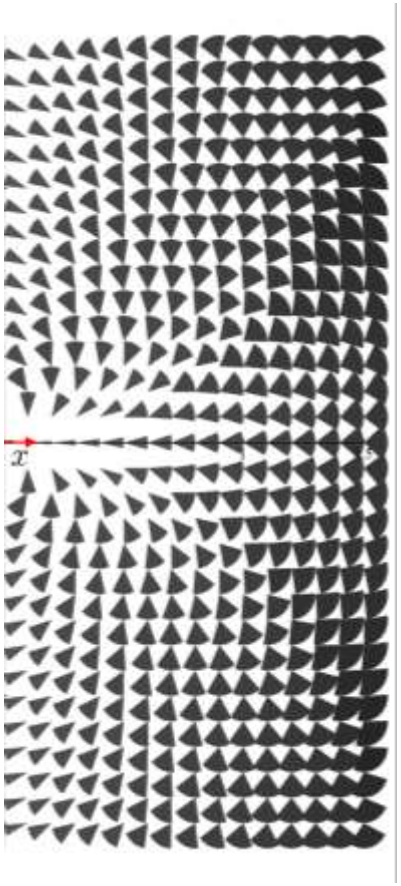

Range of the exponential map of $\mathbf{P}_{\mathrm{Curve}}(\mathbb{R}^2)$:

$$\mathfrak{R} = \{\mathrm{Exp}(\lambda_0, t) | t \leq t_{cusp}(\lambda_0)\}$$

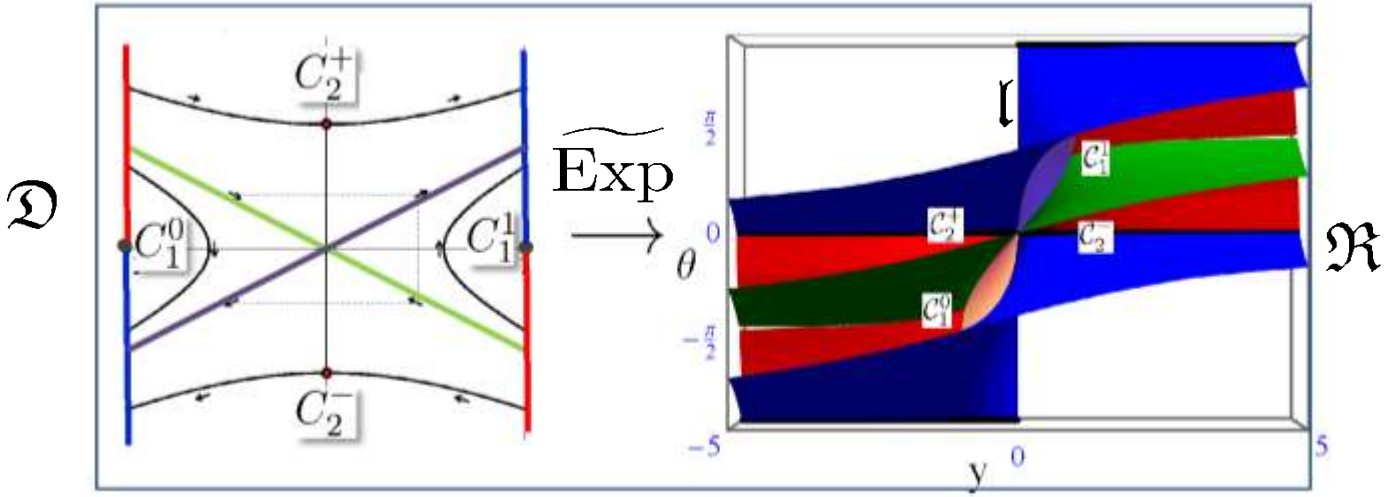

$$t_{\mathrm{cut}} \geq t_{\mathrm{cusp}}$$

R. Duits, U. Boscain, F. Rossi and Yu. L. Sachkov:
Association Fields via Cuspless Sub-Riemannian Geodesics in SE(2), JMIV, 2014.

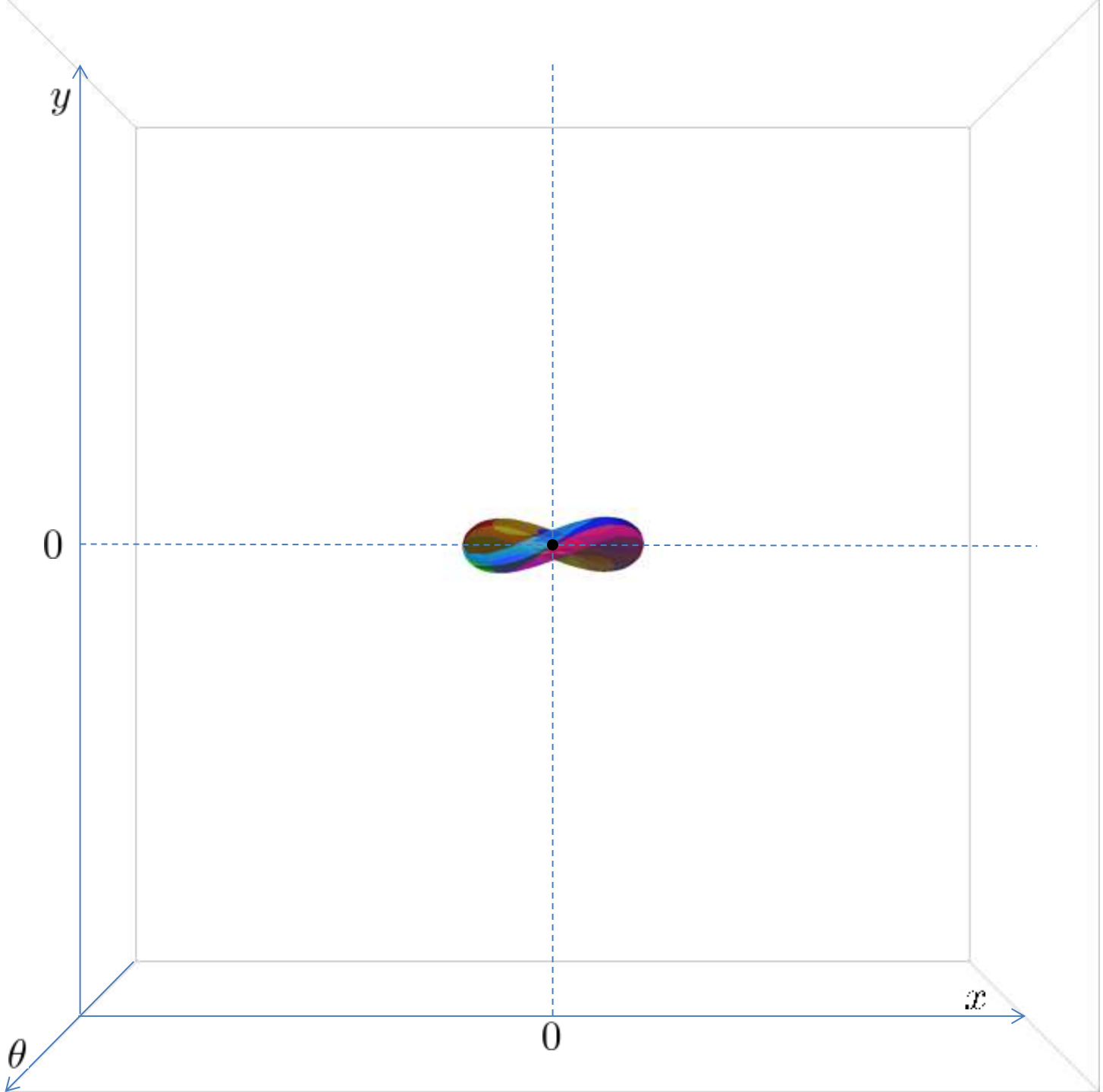
y
0
x
0
θ

Data-driven Sub-Riemannian Geodesics in SE(2)

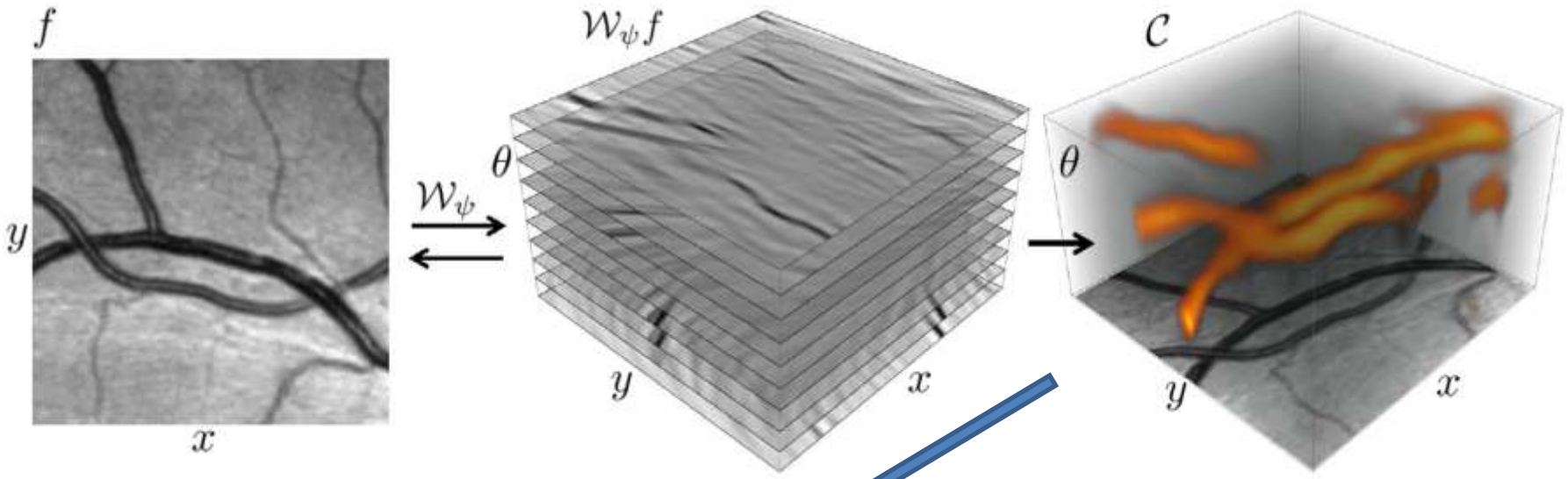

$$l = \int_0^{t_1} \mathcal{C}(x(t), y(t), \theta(t)) \sqrt{\xi^2 u_1^2(t) + u_2^2(t)}\, dt \to \min,$$

$$\mathcal{C}(\mathbf{x}, \theta) = \delta + (1 - \delta) e^{-\lambda \mathcal{V}(\mathbf{x}, \theta)}, \quad \lambda > 0, \quad \mathbf{x} = (x, y),$$

$$\mathcal{V}(\mathbf{x}, \theta) = \left| \frac{\mathcal{W}_\psi f(\mathbf{x}, \theta)}{\|\mathcal{W}_\psi f\|_\infty} \right|^p, \; p > 1, \qquad \psi \text{ - anisotropic cake wavelets,}$$

$$(\mathcal{W}_\psi f)(\mathbf{x}, \theta) = \int_{\mathbb{R}^2} \overline{\psi(R_\theta^{-1}(\mathbf{y} - \mathbf{x}))} f(\mathbf{y}) d\mathbf{y}.$$

Problem Formulation

SR-manifold $(SE(2), \Delta = \text{span}\{\mathcal{A}_1, \mathcal{A}_2\}, G^{\mathcal{C}})$, where

$$G^{\mathcal{C}}|_{\gamma(t)}(\dot\gamma(t), \dot\gamma(t)) = \mathcal{C}^2(\gamma(t)) \left(\xi^2 |\dot x(t) \cos\theta(t) + \dot y(t) \sin\theta(t)|^2 + |\dot\theta(t)|^2 \right),$$

with $\gamma : \mathbb{R} \to SE(2)$ a smooth curve, $\xi > 0$ constant, and

$$\mathcal{C} : SE(2) \to [\delta, 1], \delta > 0 \text{ is a } \textit{given external smooth cost}.$$

Optimal Control Problem:

$$\dot\gamma = u^1 \, \mathcal{A}_1|_\gamma + u^2 \, \mathcal{A}_2|_\gamma \,,$$
$$\gamma(0) = \text{Id}, \qquad \gamma(T) = g,$$
$$l(\gamma(\cdot)) = \int_0^T \mathcal{C}(\gamma(t)) \sqrt{\xi^2 |u^1(t)|^2 + |u^2(t)|^2} \, \mathrm{d}t \to \min,$$
$$\gamma(t) \in \text{SE(2)}, \quad (u^1(t), u^2(t)) \in \mathbb{R}^2, \quad \xi > 0.$$

Define $\mathcal{L}_g \phi(h) = \phi(g^{-1}h)$ then $G^{\mathcal{C}}|_\gamma(\dot\gamma, \dot\gamma) = G^{\mathcal{L}_g \mathcal{C}}\big|_{g\gamma}\left((L_g)_* \dot\gamma, (L_g)_* \dot\gamma \right)$.
Thus, $G^{\mathcal{C}}$ is not left-invariant, but shifting the cost restrict to $\gamma(0) = \text{Id}$.

Motivation of Including of External Cost

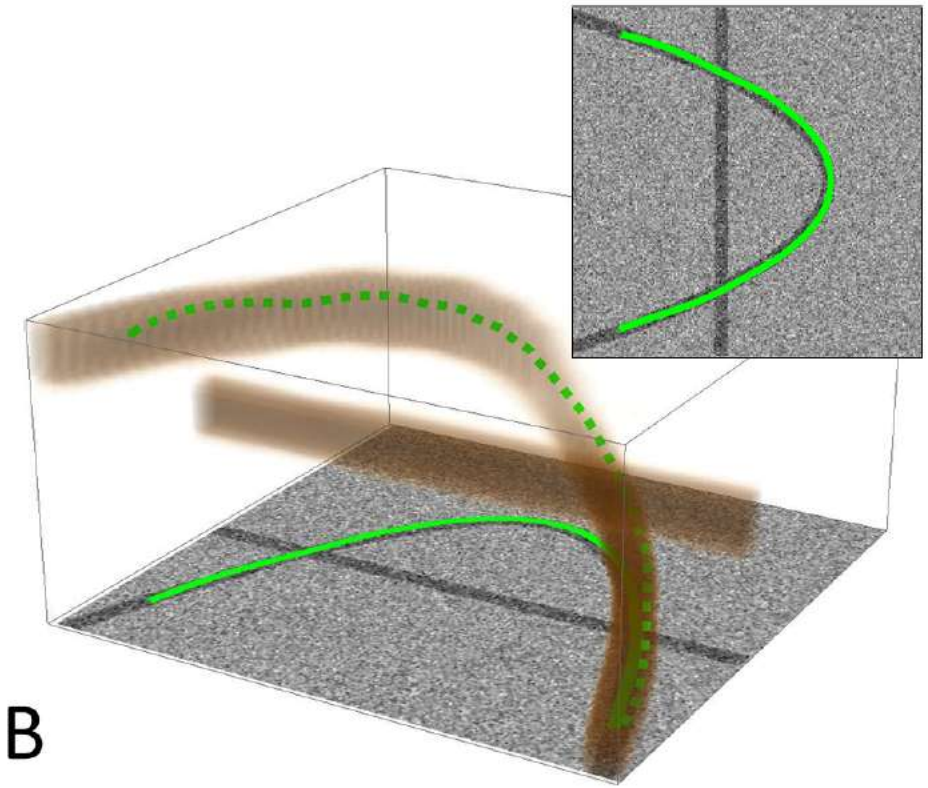

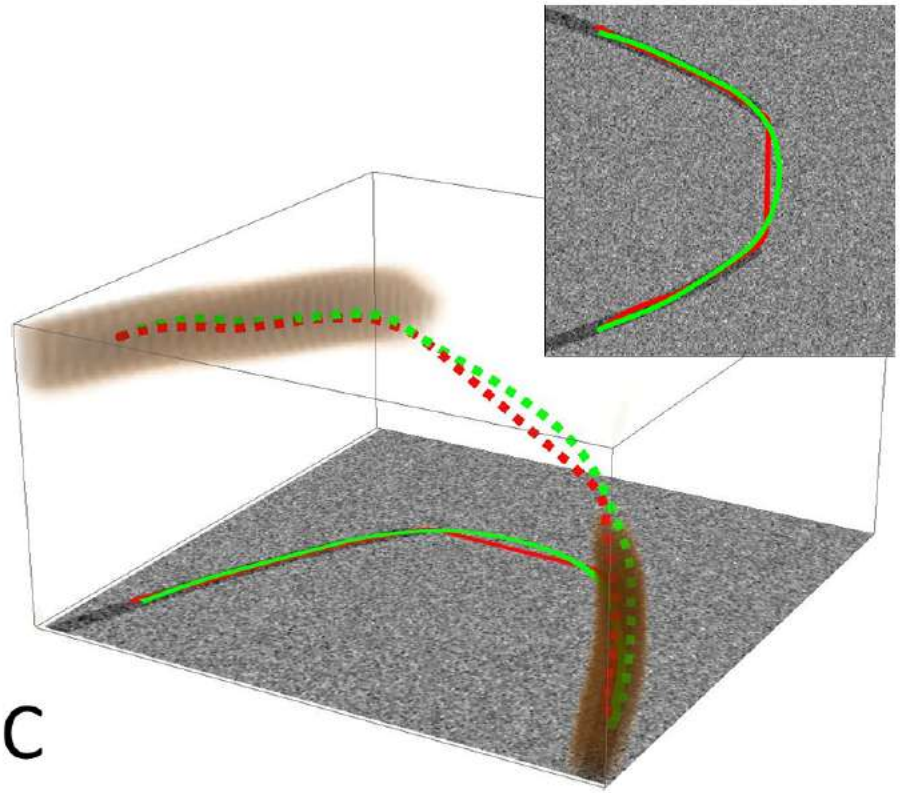

$$l = \int_0^{t_1} \mathcal{C}(x(t), y(t), \theta(t)) \sqrt{\xi^2 u_1^2(t) + u_2^2(t)}\, dt \to \min$$

ODE-based Approach

By Cauchy-Schwarz: $J = \frac{1}{2}\int_0^T \mathcal{C}^2(\gamma(t))(\xi^2|u^1(t)|^2 + |u^2(t)|^2)\,\mathrm{d}t \to \min.$

Pontryagin function: $H_u(p,g) = u^1 h_1(p,g) + u^2 h_2(p,g) - \frac{1}{2}\mathcal{C}^2(g)\left(\xi^2|u^1|^2 + |u^2|^2\right).$

Hamiltonian: $H^{fix}(g,p) = \dfrac{1}{2\,\mathcal{C}^2(g)}\left(\dfrac{h_1^2}{\xi^2} + h_2^2\right).$

Extremal controls: $u^1(t) = \dfrac{h_1(t)}{\mathcal{C}^2(\gamma(t))\xi^2}, \quad u^2(t) = \dfrac{h_2(t)}{\mathcal{C}^2(\gamma(t))}.$

Hamiltonian system:

$$\begin{cases} \dot h_1 = \frac{1}{\mathcal{C}(\gamma(\cdot))}\,\mathcal{A}_1|_{\gamma(\cdot)}\,\mathcal{C} + \frac{h_2 h_3}{\mathcal{C}^2(\gamma(\cdot))}, \\ \dot h_2 = \frac{1}{\mathcal{C}(\gamma(\cdot))}\,\mathcal{A}_2|_{\gamma(\cdot)}\,\mathcal{C} - \frac{h_1 h_3}{\xi^2\mathcal{C}^2(\gamma(\cdot))}, \\ \dot h_3 = \frac{1}{\mathcal{C}(\gamma(\cdot))}\,\mathcal{A}_3|_{\gamma(\cdot)}\,\mathcal{C} - \frac{h_2 h_1}{\mathcal{C}^2(\gamma(\cdot))}, \end{cases} \qquad \begin{cases} \dot x = \frac{h_1}{\mathcal{C}^2(\gamma(\cdot))\xi^2}\cos\theta, \\ \dot y = \frac{h_1}{\mathcal{C}^2(\gamma(\cdot))\xi^2}\sin\theta, \\ \dot\theta = \frac{h_2}{\mathcal{C}^2(\gamma(\cdot))}. \end{cases}$$

Integration of this system is a very difficult task.
No method to obtain analytic formulas of solution for general C.
ODE-based approach stops here.

PDE-based Approach

1. Derivation of HJB equation for propagation of geodesically equidistant surfaces;
2. Computing a distance map by numerical solution of BVP for HJB eq. describing propagation of geodesically equidistant surfaces;
3. Computing a minimizing geodesic satisfying boundary conditions by backward integration of Hamiltonian system.

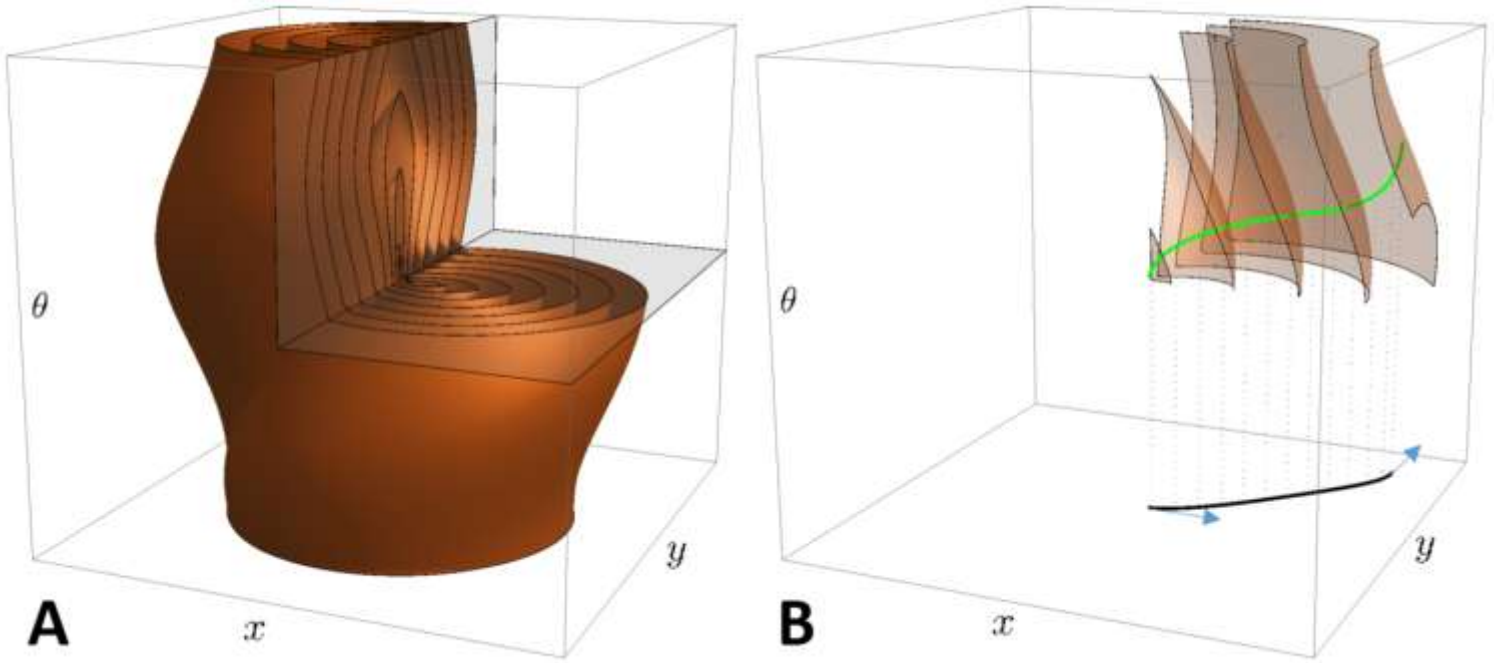

Geodesically Equidistant Surfaces

Definition *Given* $W : SE(2) \times \mathbb{R}^+ \to \mathbb{R}$ *continuous. Given a Lagrangian* $L(\gamma(r), \dot{\gamma}(r))$ *on the SR manifold* $(SE(2), \Delta, G^{\mathcal{C}})$, *with* $L(\gamma, \cdot)$ *convex. Then the family of surfaces*

$$\mathcal{S}_r := \{g \in SE(2) \mid W(g, r) = W_0(r)\}, \text{ with}$$

$W_0 : \mathbb{R} \to \mathbb{R}$ *monotonic, smooth, is geodesically equidistant if* $L(\gamma(r), \dot{\gamma}(r)) = W_0'(r)$.

Lemma *Let* L *be non-homogeneous and* $\lim_{|v| \to \infty} \frac{L(\cdot, v)}{|v|} = \infty$. *Then* $\{\mathcal{S}_r\}_{r \in \mathbb{R}}$ *is geodesically equidistant iff* W *satisfies the HJB-equation:*

$$\boxed{\frac{\partial W}{\partial r}(g, r) = -H(\mathrm{d}^{SR} W(g, r))}, \text{ with}$$

$$\mathrm{d}^{SR} W(g, r) = \mathbb{P}^*_{\Delta} \mathrm{d} W(g, r) = \sum_{i=1}^{2} \mathcal{A}_i W(g, r) \; \omega^i \big|_g .$$

Here $\mathbb{P}^*_{\Delta}(p = \sum_{i=1}^{3} h_i \, \omega^i) = \sum_{i=1}^{2} h_i \, \omega^i$ *is a dual projection with dual basis* ω^i, *and Hamiltonian* $H(\gamma, p) = \max_{v \in T_\gamma(SE(2))} \{\langle p, v \rangle - L(\gamma, v)\}$.

Viscosity Solution of HJB equation

Definition *W is viscosity solution of $\frac{\partial W}{\partial r} = -H(\mathrm{dW})$ if it is a weak solution such that for all smooth $V : (SE(2) \times \mathbb{R}) \to \mathbb{R}$ one has*

- *if $W - V$ attains a local maximum at (g_0, t_0) then $\left(\frac{\partial V}{\partial r} + H(\mathrm{dV})\right)\Big|_{(g_0,t_0)} \leq 0$,*
- *if $W - V$ attains a local minimum at (g_0, t_0) then $\left(\frac{\partial V}{\partial r} + H(\mathrm{dV})\right)\Big|_{(g_0,t_0)} \geq 0$.*

L.C. Evans, Partial Differential Equations. Graduate Studies in Mathematics, 1998.

A. Bressan, Viscosity Solutions of Hamilton-Jacobi Equations and Optimal Control Problems. Lecture Notes Dep. of Math., Pennsylvania State University, 2011.

Expression HJB in Eikonal form

Lemma *The family of surfaces $\mathcal{S}_t := \{g \in SE(2) \mid \mathfrak{W}(g) = t\}$ is geodesically equidistant w.r.t. homogeneous Lagrangian $L(\gamma, \dot{\gamma}) = \sqrt{G^{\mathcal{C}}|_{\gamma}(\dot{\gamma}, \dot{\gamma})}$, iff $\mathfrak{W}$ satisfies:*

$$\frac{1}{\mathcal{C}}\sqrt{\xi^{-2}|\mathcal{A}_1\mathfrak{W}|^2 + |\mathcal{A}_2\mathfrak{W}|^2} = 1.$$

Solutions via Data-driven Wavefront Propagation

Theorem 1 *Let $\mathfrak{W}(g)$ be a solution of the BVP*

$$\begin{cases} \sqrt{(\mathcal{C}(g))^{-2}\left(\xi^{-2}|\mathcal{A}_1\mathfrak{W}(g)|^2 + |\mathcal{A}_2\mathfrak{W}(g)|^2\right)} - 1 = 0, \ \textit{for } g \neq e, \\ \mathfrak{W}(e) = 0. \end{cases}$$

Then the iso-surfaces

$$\mathcal{S}_t = \{g \in SE(2) \mid \mathfrak{W}(g) = t\}$$

are geodesically equidistant with unit speed.

A SR geodesic departing from $g \in SE(2)$ is found by backward integration

$$\dot{\gamma}_b(t) = -\frac{\mathcal{A}_1\mathfrak{W}|_{\gamma_b(t)}}{(\xi\,\mathcal{C}(\gamma_b(t)))^2}\,\mathcal{A}_1|_{\gamma_b(t)} - \frac{\mathcal{A}_2\mathfrak{W}|_{\gamma_b(t)}}{(\mathcal{C}(\gamma_b(t)))^2}\,\mathcal{A}_2|_{\gamma_b(t)}\,, \qquad \gamma_b(0) = g.$$

Accepted to SSVM; Submitted to SIAM

Implementation of Solution to the BVP

Iterative implementation to solve BVP:

- Viscosity solutions of subsequent IVP's for each $r \in [r_0, r_0 + \epsilon]$, with $r_0 = n\epsilon$ at step $n \in \mathbb{N} \cup \{0\}$, $\epsilon > 0$ fixed:

$$\begin{cases} \frac{\partial W^\epsilon}{\partial r}(g,r) & = 1 - \sqrt{(\mathcal{C}(g))^{-2}\left(\xi^{-2}|\mathcal{A}_1 W^\epsilon(g,r)|^2 + |\mathcal{A}_2 W^\epsilon(g,r)|^2\right)}, \\ W^\epsilon(g,r_0) & = W^\epsilon_{r_0}(g). \end{cases}$$

Here $W^\epsilon_{r_0=0} = \delta^M_e$ the morphological delta.

- After each iteration at time-step $r = r_0$, update $W^\epsilon(e,r_0) = W^\epsilon_{r_0}(e) = 0$.

For $g \neq e$ and $n \geq 1$ we set $W^\epsilon_{r_0}(g) = W^\epsilon_{r_0-\epsilon}(g, r_0)$.

- Then we obtain

$$\mathfrak{W}(g) = W^\infty(g) = \lim_{\epsilon \to 0} \lim_{n \to \infty} W^\epsilon(g, n\epsilon),$$

which satisfies

$$\begin{cases} \sqrt{(\mathcal{C}(g))^{-2}\left(\xi^{-2}|\mathcal{A}_1 \mathfrak{W}(g)|^2 + |\mathcal{A}_2 \mathfrak{W}(g)|^2\right)} - 1 = 0, \text{ for } g \neq e, \\ \mathfrak{W}(e) = 0. \end{cases}$$

Solutions via Wavefront Propagation for C=1

Theorem 2 *Let $\mathfrak{W}(g)$ be the viscosity solution of BVP:*

$$\begin{cases} \sqrt{\xi^{-2}|\mathcal{A}_1\mathfrak{W}(g)|^2 + |\mathcal{A}_2\mathfrak{W}(g)|^2} - 1 = 0, \ \textit{for } g \neq e, \\ \mathfrak{W}(e) = 0. \end{cases}$$

Then $\mathcal{S}_t = \{g \in SE(2) \mid \mathfrak{W}(g) = t\}$ equals the SR-sphere of radius t. Backward integration gives optimal geodesics reaching e at $t = d(g,e) :=$

$$\min_{\substack{\gamma \in C^\infty(\mathbb{R}^+, SE(2)), T \geq 0, \\ \dot\gamma \in \Delta, \gamma(0) = e, \gamma(T) = g}} \int_0^T \sqrt{|\dot\theta(t)|^2 + \xi^2 |\dot x(t)\cos\theta(t) + \dot y(t)\sin\theta(t)|^2}\, \mathrm{d}t.$$

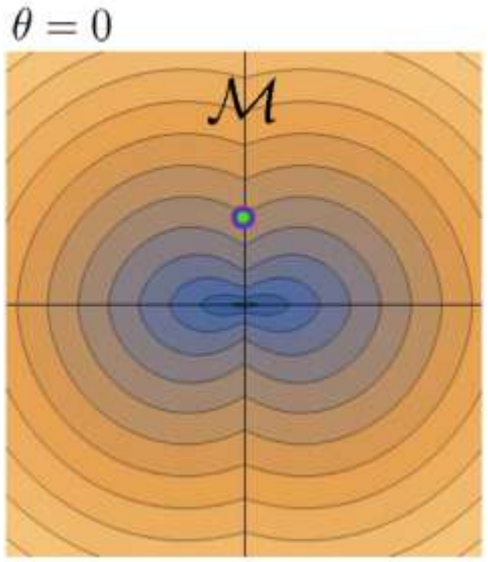

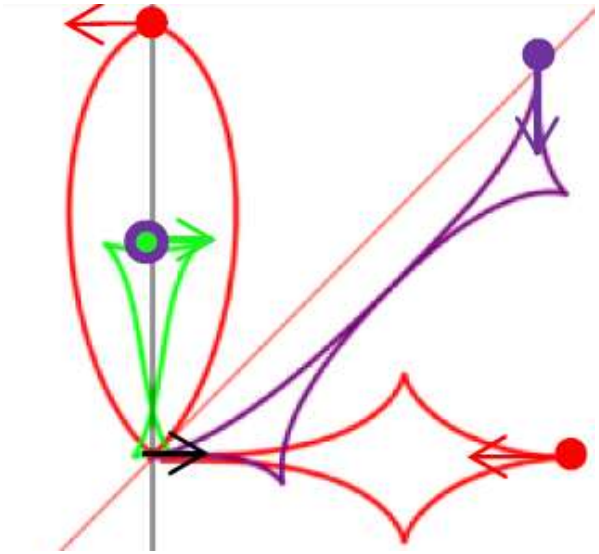

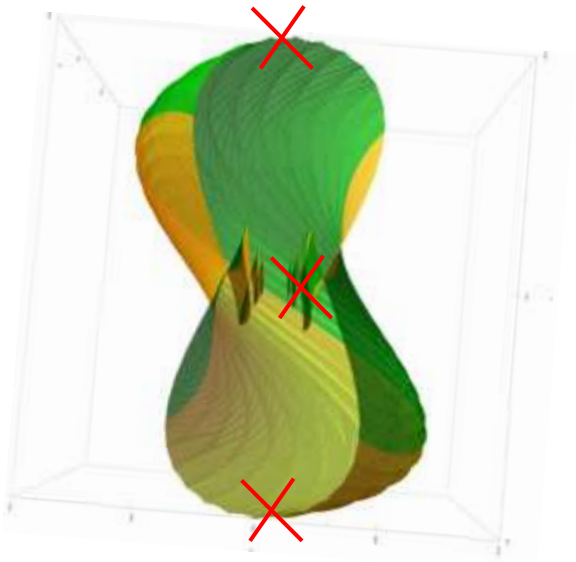

Solutions given by algorithm do not pass first Maxwell set and conjugate locus

Numerical Verification for C=1

Converging to Exact Geodesics

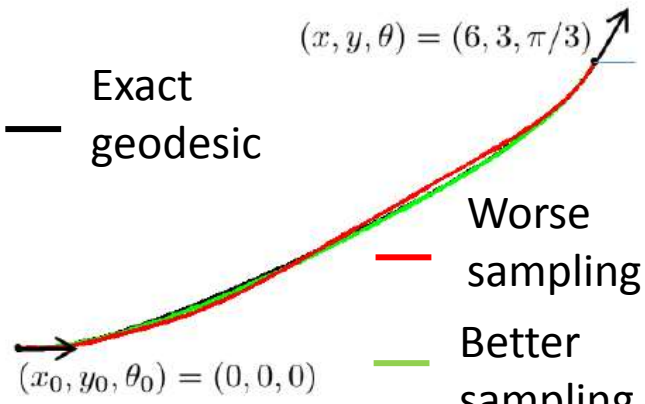

SR-sphere Numerically

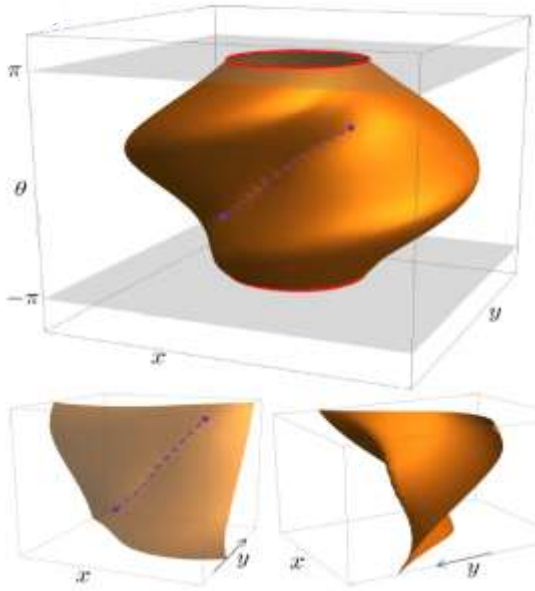

Exact Wavefront

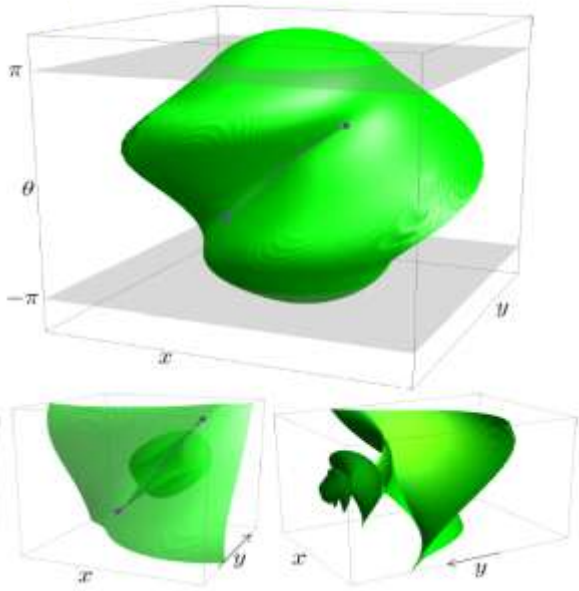

Max Absolute Error

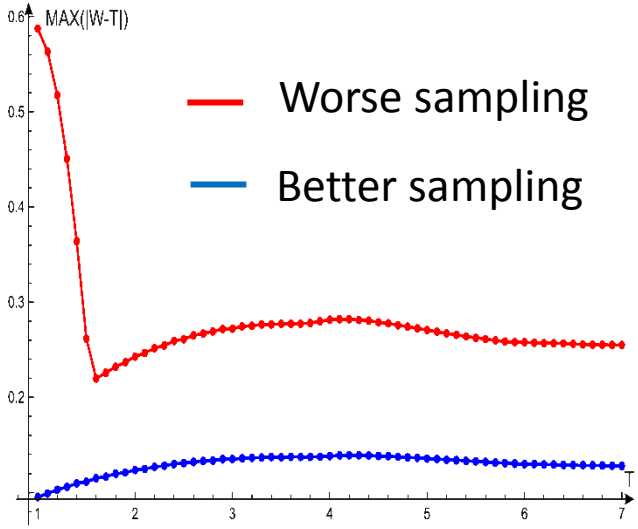

(T – radius of SR-sphere)

Maxwell Set Exact

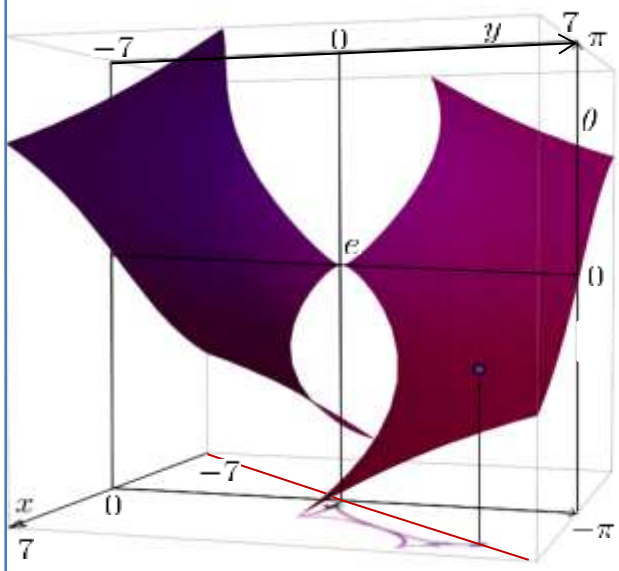

Maxwell Set Numerically

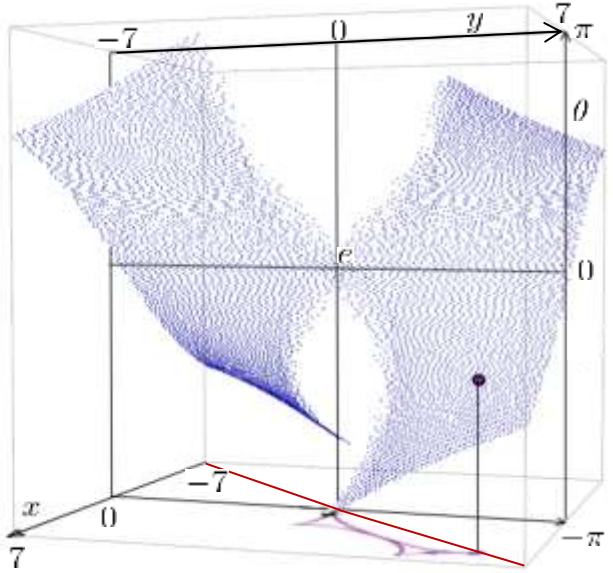

Application in Retinal Imaging

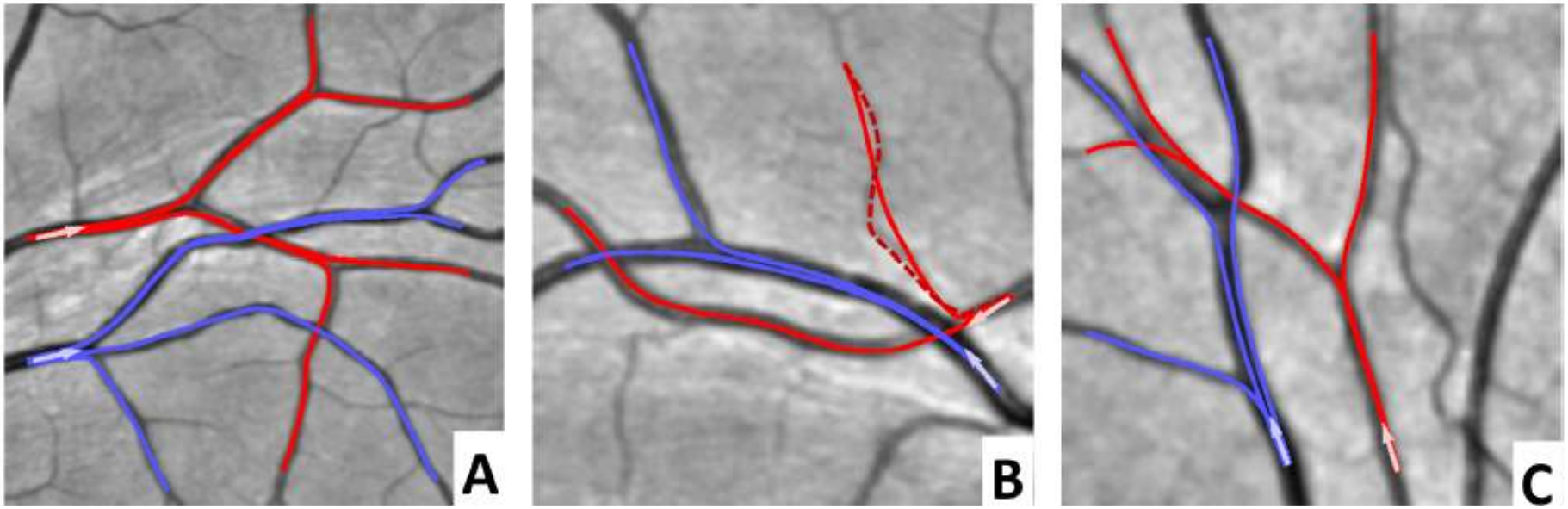

Tests on image patches exhibiting crossings:

1) Two seed points were selected manually (for artery and vein),
2) For each seed point the value function W was calculated,
3) Multiple end-points were traced back to the seed point.

Values of parameters in cost function: $p = 3,\ \delta = 0.3,\ \lambda = 30$

Solid curves: $\xi = 0.1$ Dashed curves: $\xi = 0.5$

Comparison with Classical Methods

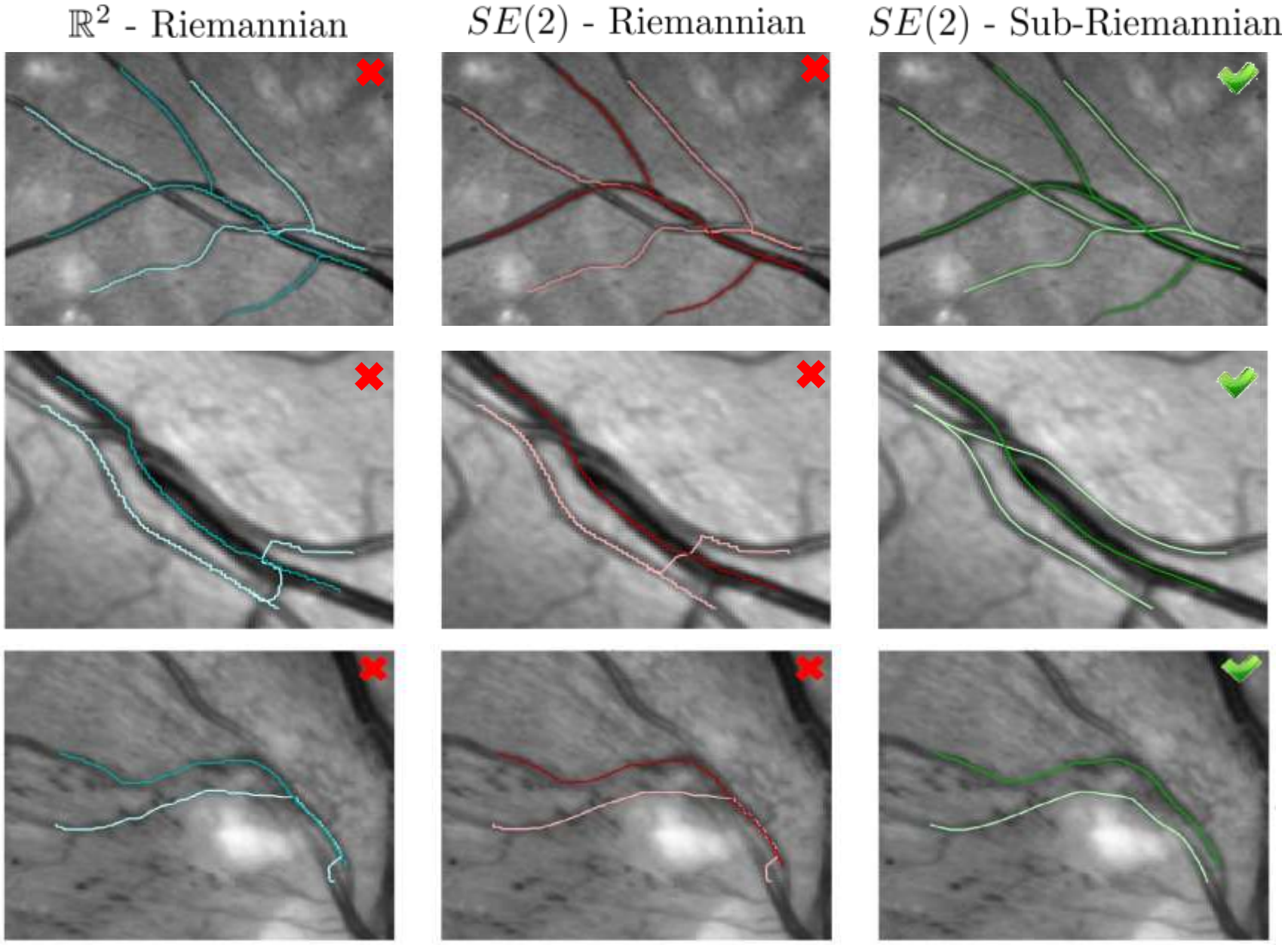

Summary: Data-driven SR-Geodesics in SE(2)

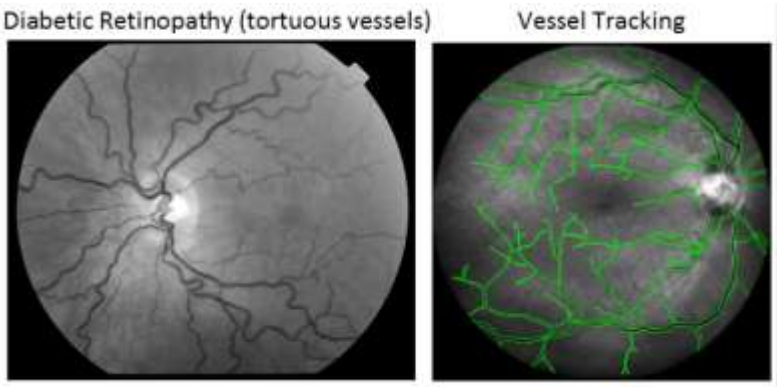

Results of vessel tracking by data-driven SR-geodesics

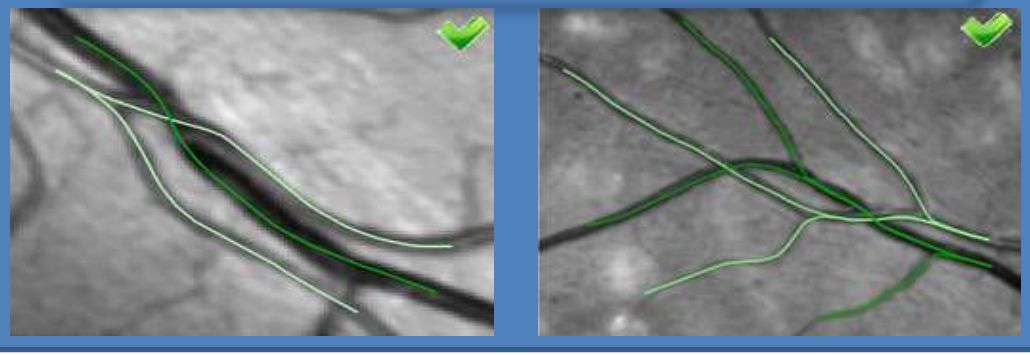

External cost $\mathcal{C}$ from image f:

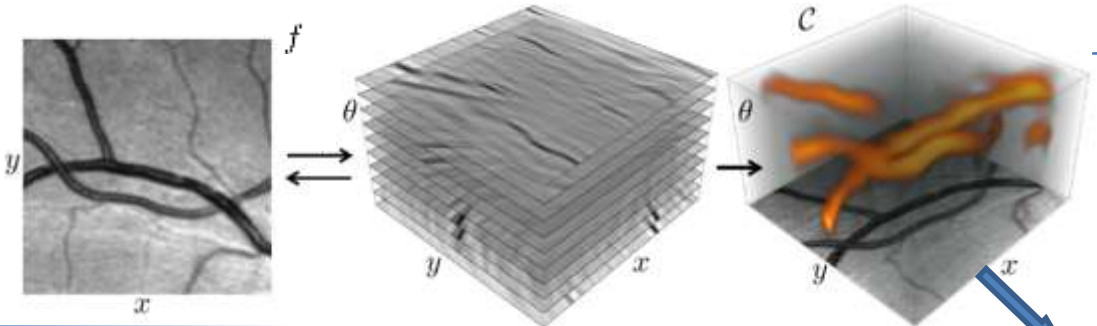

$$(x, y, \theta) \in \mathrm{SE}(2) = \mathbb{R}^2 \rtimes S^1,$$

Problem formulation:

$$\dot{\gamma} = u_1 \overbrace{(\cos\theta\partial_x + \sin\theta\partial_y)}^{\mathcal{A}_1} + u_2 \overbrace{\partial_\theta}^{\mathcal{A}_2},$$
$$\gamma(0) = e, \quad \gamma(T) = g \in \mathrm{SE}(2),$$
$$(u_1(t), u_2(t)) \in \mathbb{R}^2,$$

Propagation of SR-spheres via HJB system:

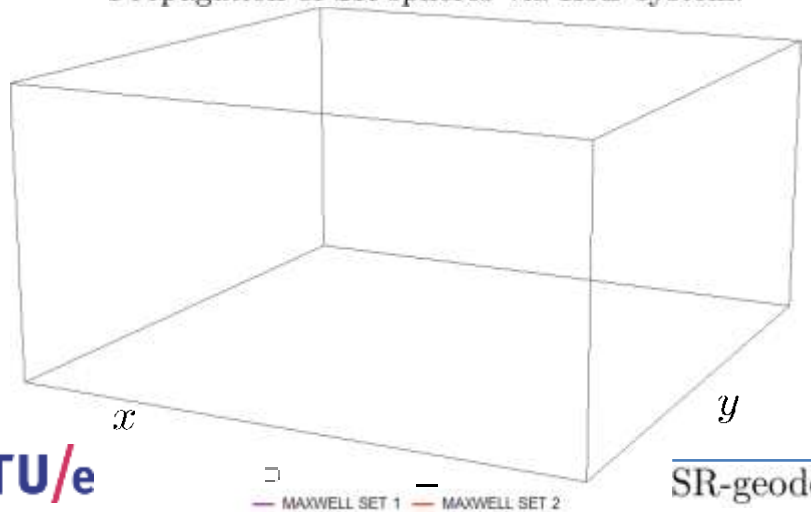

$$l = \int_0^T \mathcal{C}(x(t), y(t), \theta(t)) \sqrt{\xi^2 u_1^2(t) + u_2^2(t)}\, dt \to \min.$$

SR-distance from the unity $e = (0, 0, 0)$:

$$W(g) := \inf\{l(\gamma(t)) \,|\, \gamma(0) = e, \gamma(T) = g,$$
$$\dot{\gamma}(t) \in \mathrm{span}\{\mathcal{A}_1|_{\gamma(t)}, \mathcal{A}_2|_{\gamma(t)}\} \text{ a.e. in } [0, T]\}.$$

$W(g)$ must satisfy HJB system:

$$\begin{cases} \sqrt{(\xi^{-2}|\mathcal{A}_1 W(g)|^2 + |\mathcal{A}_2 W(g)|^2)} = \mathcal{C}(g), \text{ for } g \neq e, \\ W(e) = 0, \end{cases}$$

SR-geodesics by steepest decent on $W(g)$ in horizontal directions $\mathcal{A}_1$, $\mathcal{A}_2$

Data-driven SR-Geodesics in SE(2): Results and Plans

Results: new PDE-based approach, that is

- Fast and accurate for C=1,
- **Allows fast adaptation for general C,**
- At least for C=1 provides the global minimizers
  and stays away from both Maxwell and conjugate points,
- Shows promising results in retinal vessel tracking.

Plans:

- Adapt to other 3D Lie groups SL(2), SO(3), H(3) and SH(2)
- Complete vascular tree segmentation via SR Fast Marching,
- Adapt to Lie group SE(3).

Sub-Riemannian problem in SO(3) with cuspless spherical projection constraint

(A. Mashtakov, R. Duits, Y.L. Sachkov, I. Beschastnyi)

Association Field Model on the Retinal Sphere

Statement of the problem **$P_{curve}(S^2)$**:

Given $\xi > 0, \quad \mathbf{n}_i \in S^2, \ i \in \{0,1\},$
$\mathbf{n}_i' \in T_{\mathbf{n}_i} S^2, \quad \|\mathbf{n}_i'\| = 1.$

Find a smooth curve $\gamma : [0, l] \to S^2$ s. t.:

$$\gamma(0) = \mathbf{n}_0, \quad \gamma(l) = \mathbf{n}_1,$$
$$\gamma'(0) = \mathbf{n}_0', \quad \gamma'(l) = \mathbf{n}_1',$$
$$E(\gamma(\cdot)) = \int_0^l \sqrt{\xi^2 + k_g^2(s)}\, \mathrm{d}s \to \min,$$

where

$$k_g(s) = \gamma''(s) \cdot (\gamma(s) \times \gamma'(s)).$$

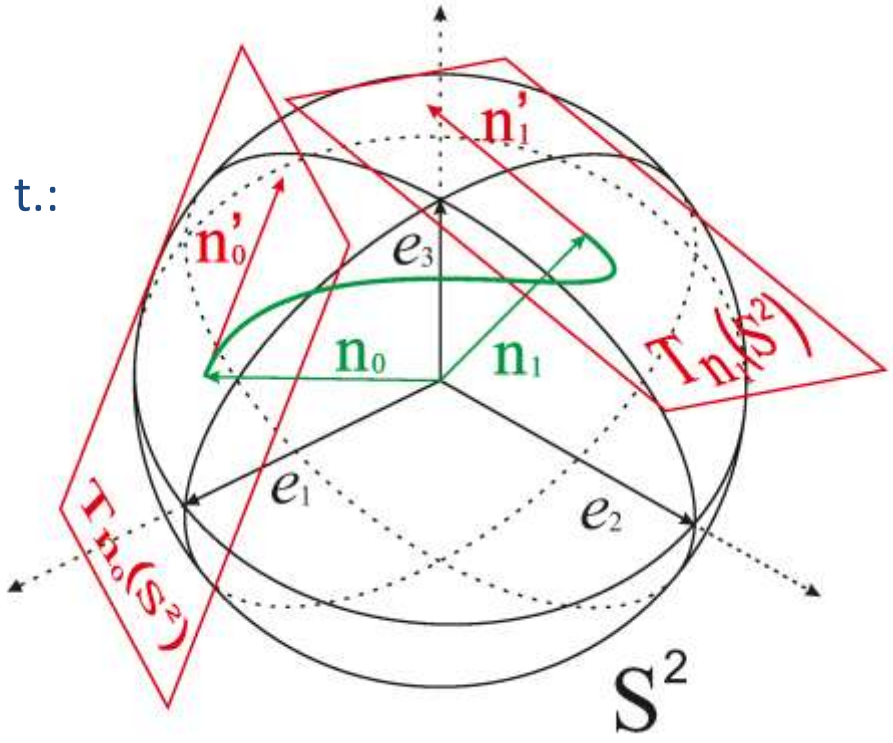

Motivation: A natural extension of a model due to J. Petitot, G. Citti and A. Sarti which additionally takes into account the spherical nature of the retina. It is important both for cortical modeling and for processing retinal images.

Pmec(S^2): Lift Pcurve(S^2) to SR-problem on SO(3)

$$\dot{R} = -u_1 R A_2 + u_2 R A_1, \quad R(0) = \mathrm{Id}, \; R(t_1) = R_1, \quad R \in \mathrm{SO}(3),$$
$$\mathfrak{E}(R(\cdot)) = \int_0^{t_1} \sqrt{\xi^2 u_1^2 + u_2^2}\, dt \to \min, \quad (u_1, u_2) \in \mathbb{R}^2, \quad \xi > 0.$$

We parameterize $\mathrm{SO}(3) \ni R(x, y, \theta) = \mathrm{e}^{yA_3}\, \mathrm{e}^{-xA_2}\, \mathrm{e}^{\theta A_1}$,
and use the map projection from $\mathrm{SO}(3) \ni R \mapsto Re_1 \in S^2$.

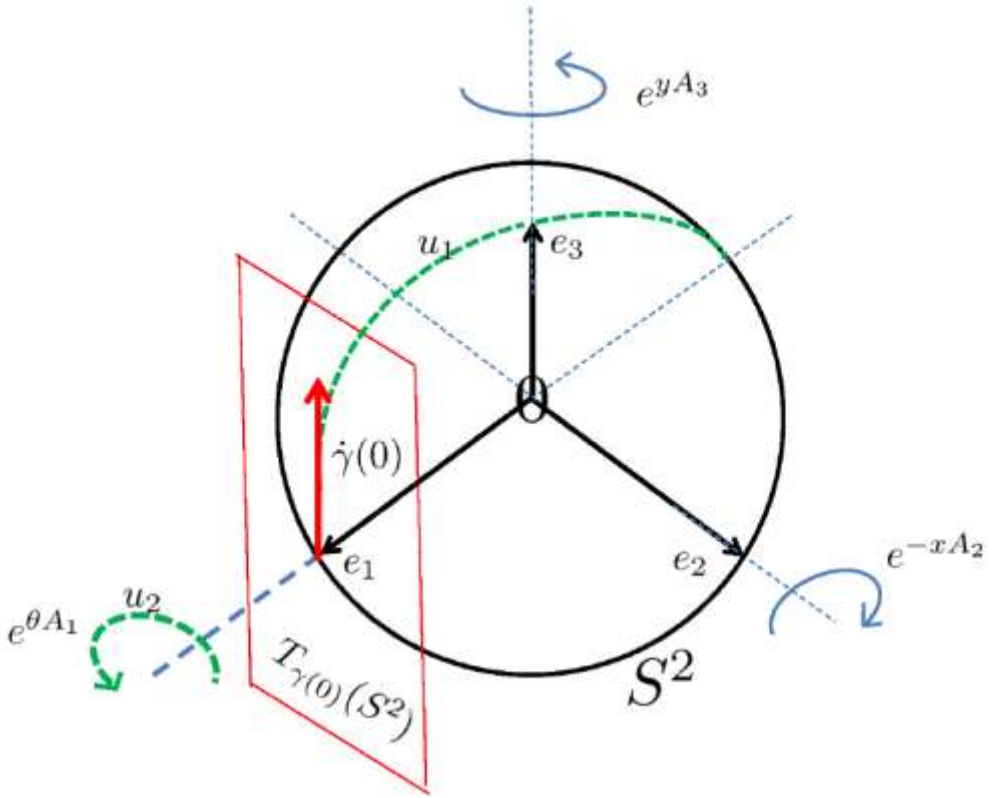

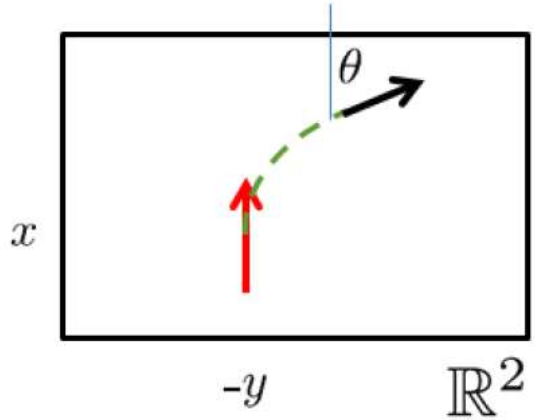

Analogy with close related sub-Riemannian problem on special Euclidean group.

Pontryagin Maximum Principle

- Left Invariant Hamiltonians $h_i = \langle \lambda, X_i \rangle$, $i = 1, 2, 3$
- Maximum Condition

$$u_1 = \frac{h_1}{\xi^2}, \qquad u_2 = h_2.$$

- The Hamiltonian system of PMP

$$\begin{cases} \dot{h}_1 = -h_2 h_3, \\ \dot{h}_2 = \frac{1}{\xi^2} h_1 h_3, \\ \dot{h}_3 = \left(1 - \frac{1}{\xi^2}\right) h_1 h_2, \end{cases} \qquad \begin{cases} \dot{x} = \frac{h_1}{\xi^2} \cos\theta, \\ \dot{y} = -\frac{h_1}{\xi^2} \sec x \sin\theta, \\ \dot{\theta} = \frac{h_1}{\xi^2} \sin\theta \tan x + h_2. \end{cases}$$

vertical part horizontal part

Vertical Part in Spherical Arclength

For any $s \in [0, \mathrm{s}_{\max}(h(0)))$, $h_1(0) > 0$ the vertical part is equivalent to the following linear system:

$$\begin{cases} h_1 = \xi^2 u_1 = \xi^2 \frac{ds}{dt} \geq 0, \\ h_2'(s) = h_3(s), & h_2(0) = h_{20}, \\ h_3'(s) = (\xi^2 - 1) h_2(s), & h_3(0) = h_{30}. \end{cases}$$

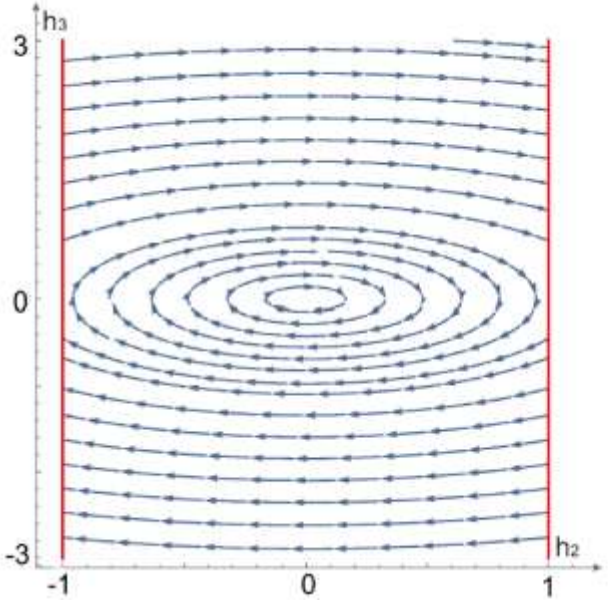

Elliptic $\xi < 1$

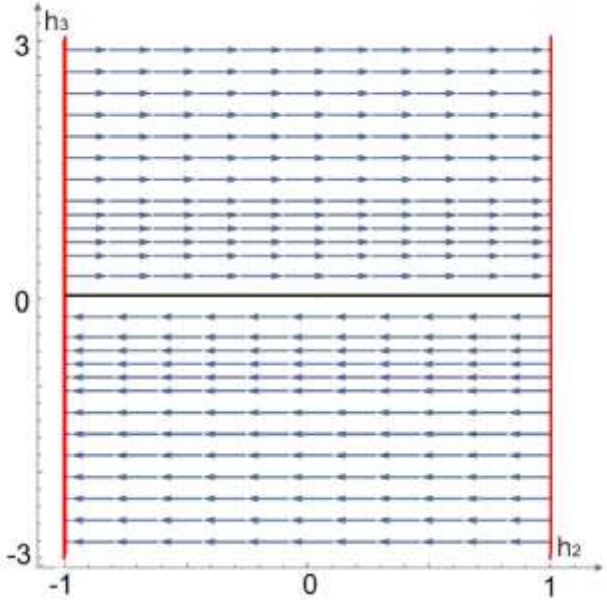

Linear $\xi = 1$

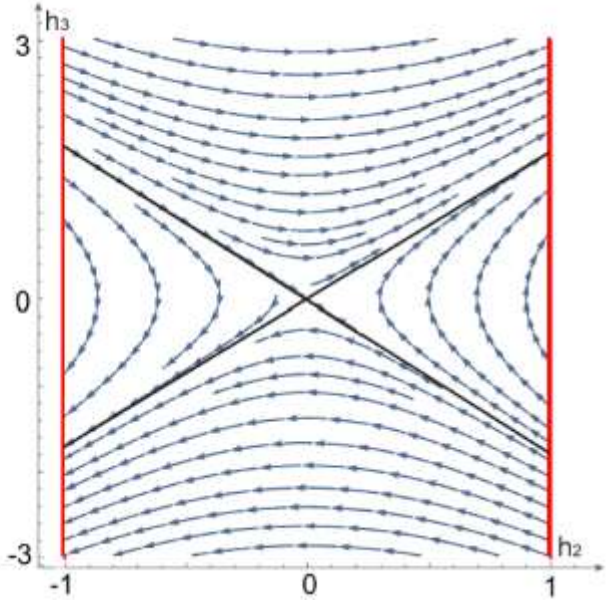

Hyperbolic $\xi > 1$

Horizontal Part

Explicit expressions in terms of Jacobi elliptic functions.

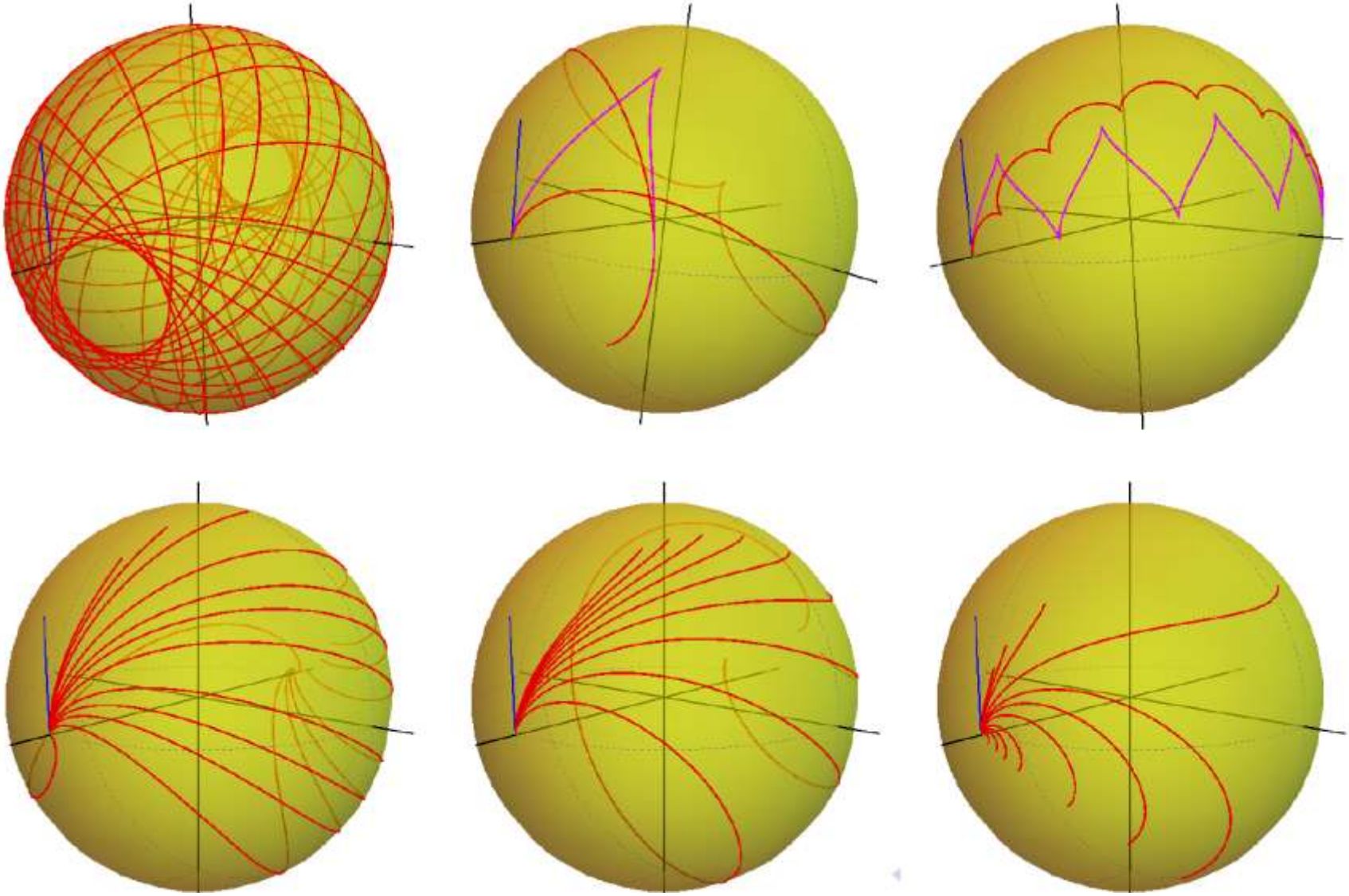

Analysis of Plots of Wave Front

$$W(T) = \{\mathrm{Exp}(\lambda_0, T) | \lambda_0 \in T^*_{\mathrm{Id}}\,\mathrm{SO}(3), \mathrm{H}(\lambda_0) = \tfrac{1}{2}\}.$$

Wave fronts in $\mathrm{P}_{\mathrm{mec}}$ in elliptic (green), linear (red) and hyperbolic (blue) cases.

Comparison with SE(2) shows local similarity of wave fronts in SE(2) and SO(3).

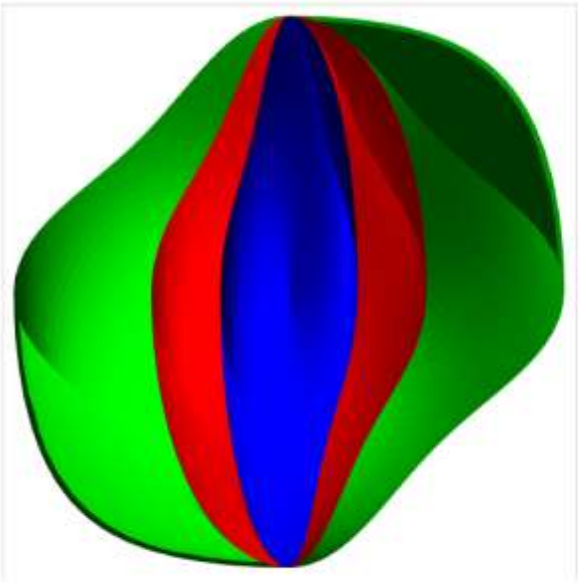

SO(3)

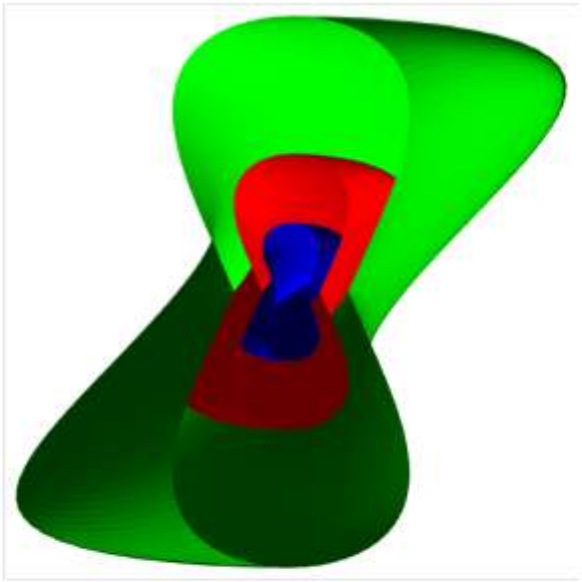

SO(3)

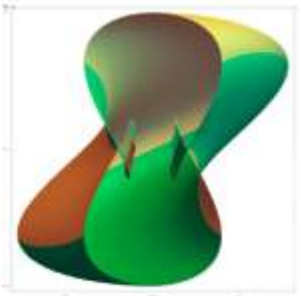

SE(2) and SO(3)

Singularities of Wavefront on SO(3)

Rotational symmetry in linear case $\xi = 1$.
Conjugate locus is a circle without a point.

For $\xi \neq 1$ the rotational symmetry is destroyed.
Conjugate and Maxwell points are getting separated and the conjugate locus has an astroidal shape.

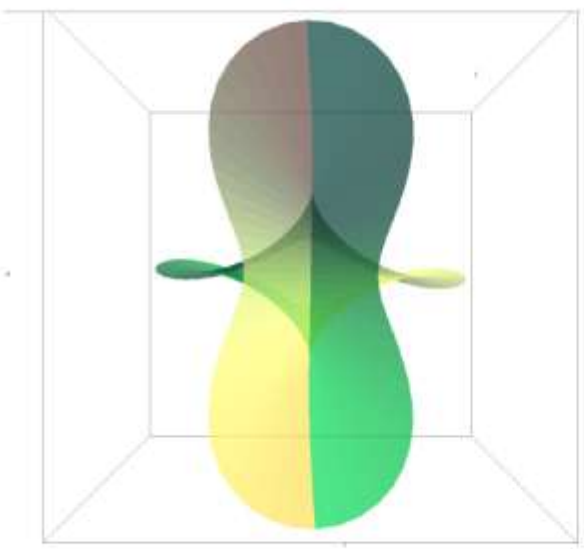

$\xi < 1$

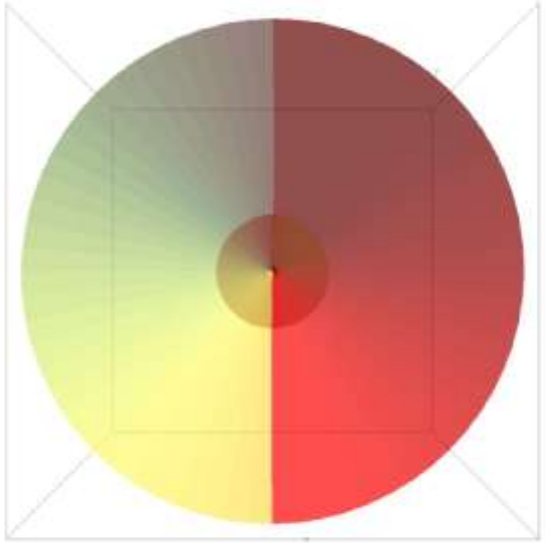

$\xi = 1$

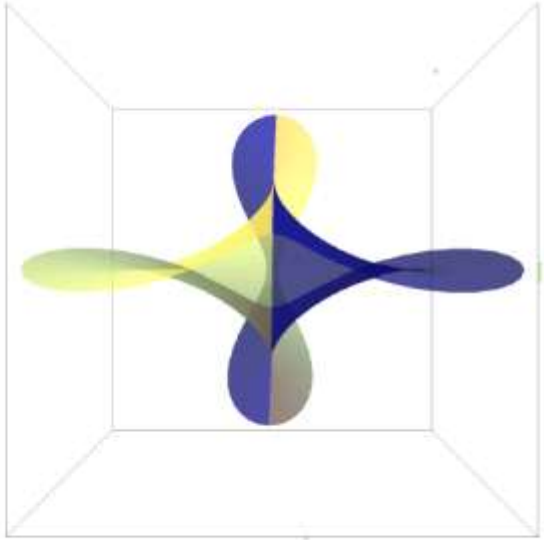

$\xi > 1$

Cusp Surfaces

Red surface: endpoints of geodesics starting from cusp.
Blue surface: endpoints of geodesics ending in cusp.

SO(3):

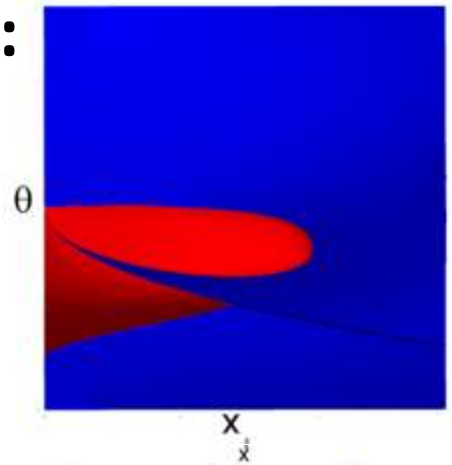

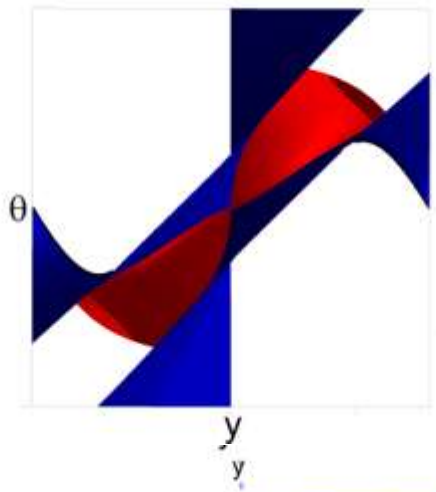

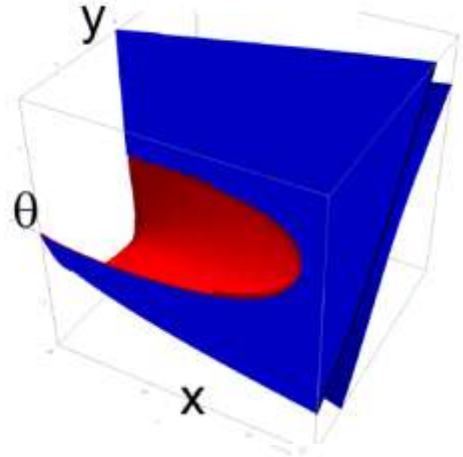

SE(2):

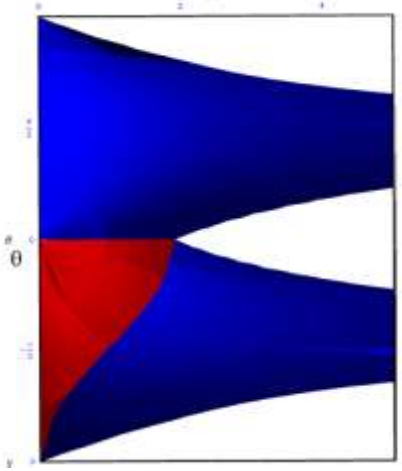

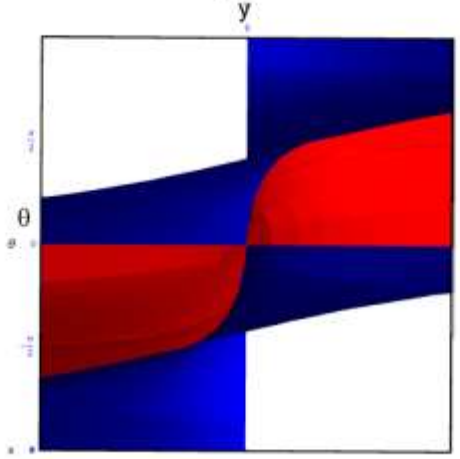

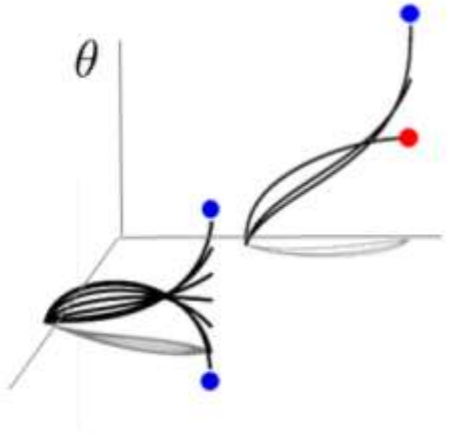

Application for Processing of Spherical Images of Retina

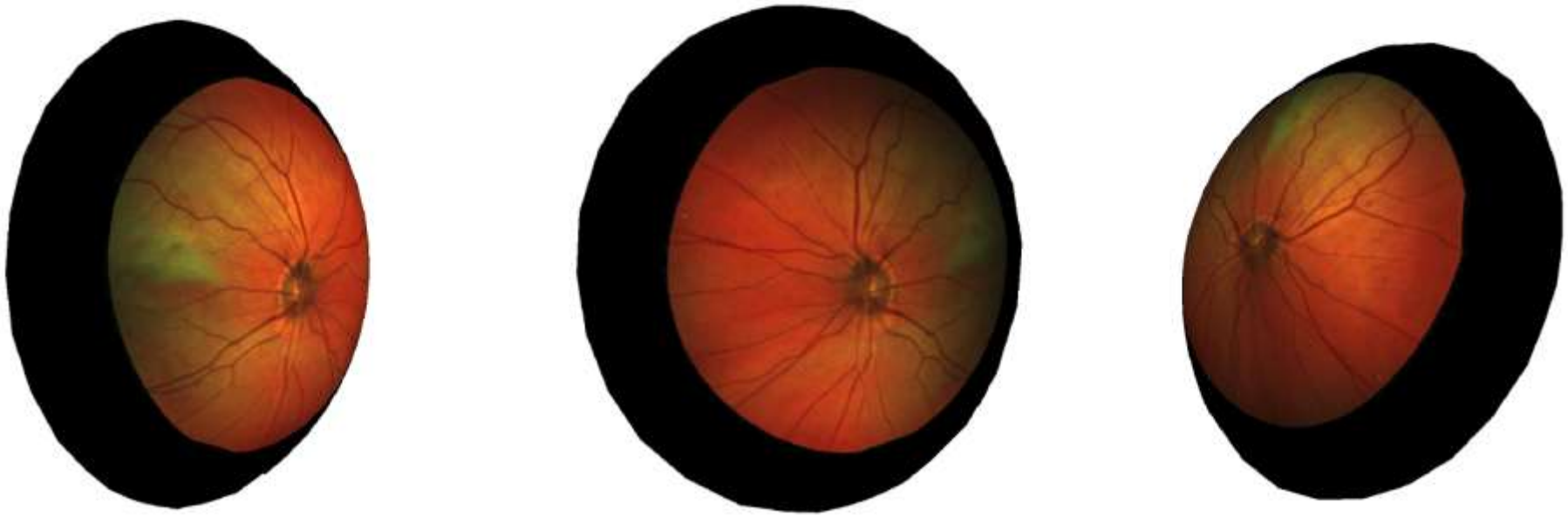

+ No distortion
+ Existence of geodesics with cuspless projections up to infinity

Sub-Riemannian geodesics in SO(3) with cuspless spherical projections: Results

The effect of ξ on cuspless S-curves.

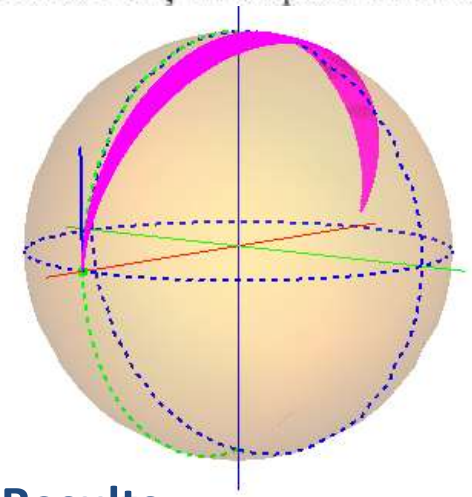

First cusp time in elliptic case

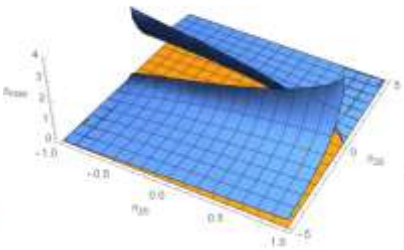

Some geodesics have no cusp

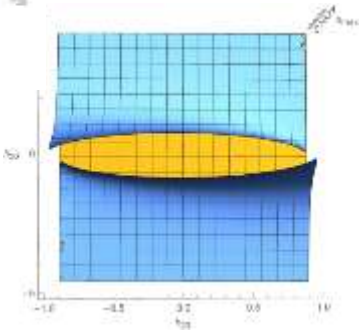

First cusp time in hyperbolic case

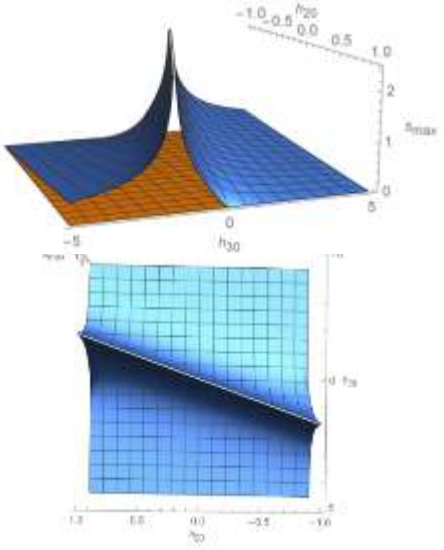

Results:

- Lift $P_{\text{curve}}(S^2)$ to sub-Riemannian problem on SO(3);
- Hamiltonian system of PMP;
- Classification by different dynamic of vertical part on elliptic ($0 < \xi < 1$), linear ($\xi = 1$) and hyperbolic ($\xi > 1$) cases;
- Explicit expressions for SR-geodesics in both SR-arclength and spherical arclength parameterization;
- Evaluation of first cusp time and asymptotic analysis & computation conjugate locus.
- Comparison cusp-surfaces and wavefronts w.r.t. SE(2)

Conclusion

Results:

- new PDE-based approach for computing SR-geodesics, that allows extension to data-driven cost
- Numerical solution to sub-Riemannian problem in SE(2) with given external cost
- Parameterization of range of exponential mapping in sub-Riemannian problem in SO(3) with cuspless spherical projections constraint

Plans:

- Adaptation to other Lie groups such as SE(3) and SO(3)
- Fast, efficient implementation using ordered upwind schemes
- Algorithm for solving BVP for geodesics with cuspless spherical projection

Thank you for your attention!